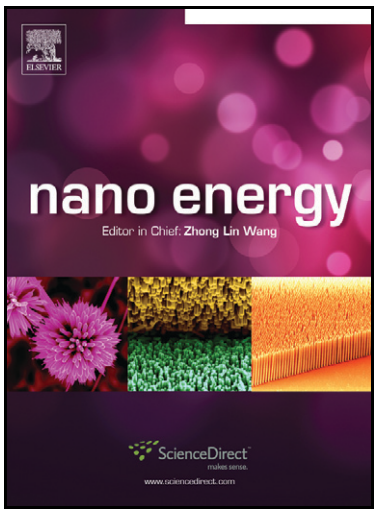

www.elsevier.com/nanoenergy

Hybrid nanostructured materials for high-performance electrochemical capacitors

Guihua Yu, Xing Xie, Lijia Pan, Zhenan Bao, Yi Cui

PII: S2211-2855(12)00211-X
DOI: http://dx.doi.org/10.1016/j.nanoen.2012.10.006
Reference: NANOEN137

To appear in: *Nano Energy*

Received date: 5 October 2012
Revised date: 16 October 2012
Accepted date: 16 October 2012

Cite this article as: Guihua Yu, Xing Xie, Lijia Pan, Zhenan Bao, Yi Cui, Hybrid nanostructured materials for high-performance electrochemical capacitors, *Nano Energy,* http://dx.doi.org/10.1016/j.nanoen.2012.10.006

Hybrid nanostructured materials for high-performance electrochemical capacitors

Guihua Yu [a], Xing Xie [b,c], Lijia Pan [d], Zhenan Bao [d,*], and Yi Cui [b,*]

[a] *Materials Science and Engineering Program and Department of Mechanical Engineering, The University of Texas at Austin, Austin, TX 78712, U.S.A.*
[b] *Department of Materials Science and Engineering, Stanford University, Stanford, CA 94305, U.S.A.*
[c] *Department of Civil and Environmental Engineering, Stanford University, Stanford, CA 94305, U.S.A.*
[d] *Department of Chemical Engineering, Stanford University, Stanford, CA 94305, U.S.A.*

Corresponding Authors: yicui@stanford.edu, *zbao@stanford.edu*

Keywords: electrochemical capacitors; hybrid nanomaterials; nanostructures; energy storage; pseudocapacitive; supercapacitors

Abstract: The exciting development of advanced nanostructured materials has driven the rapid growth of research in the field of electrochemical energy storage (EES) systems which are critical to a variety of applications ranging from portable consumer electronics, hybrid electric vehicles, to large industrial scale power and energy management. Owing to their capability to deliver high power performance and extremely long cycle life, electrochemical capacitors (ECs), one of the key EES systems, have attracted increasing attention in the recent years since they can complement or even replace batteries in the energy storage field, especially when high power delivery or uptake is needed. This review article describes the most recent progress in the development of nanostructured electrode materials for EC technology, with a particular focus on hybrid nanostructured materials that combine carbon based materials with pseudocapacitive metal oxides or conducting polymers for achieving high-performance ECs. This review starts with an overview of EES technologies and the comparison between various EES systems, followed by a brief description of energy storage mechanisms for different types of EC materials. This review emphasizes the exciting development of both hybrid nanomaterials and novel support structures for effective electrochemical utilization and high mass loading of active electrode materials, both of which have brought the energy density of ECs closer to that of batteries while still maintaining their characteristic high power density. Last, future research directions and the remaining challenges toward the rational design and synthesis of hybrid nanostructured electrode materials for next-generation ECs are discussed.

Introduction

The dramatic climate change, the limited reserves of fossil fuels, and energy security concerns, have spurred internationally unprecedented interest in developing renewable energy technologies from sustainable and renewable energy resources. In fact, there is a rapid increase in renewable energy productions from solar and wind, the most abundant and readily available resources [1-3]. Given the intermittent nature of solar and wind energy, efficient energy storage systems are critically needed to make the best of the electricity generated from these sources since they can promote the reliability and effective use of the entire power system (generation, transmission and distribution) by storing energy when in excess while releasing it when in high demand. Among various energy storage systems, the most dominant is electrochemical energy storage (EES) system, including batteries, electrochemical capacitors (ECs) and fuel cells [4, 5]. These three device systems share the "electrochemical similarities" and common features that the energy-producing processes take place at the phase boundary at the electrode/electrolyte interface. To meet the increasingly higher requirements of future systems, from portable consumer electronics, hybrid and electric vehicles, to large-scale industrial power systems, the performance of EES devices has to be substantially improved by developing new materials and better understanding of the fundamental electrochemical processes at the interface.

The key parameters to evaluate the performance of EES systems and their potential for practical applications include energy density (W h kg^{-1} or W h L^{-1}, energy stored per unit weight/volume), power density (W kg^{-1} or W L^{-1}), specific capacitance (F g^{-1}),

specific capacity (mA h g^{-1}), cycle life and calendar life, as well as cost and environmental safety [6-8]. To clearly compare the power and energy capabilities, **Figure 1** shows the Ragone plot of specific power versus specific energy for the most important EES systems. Fuel cells and batteries are often considered to be high-energy systems, while ECs (also known as supercapacitors or ultracapacitors) and conventional electrostatic capacitors are considered to be high-power systems.

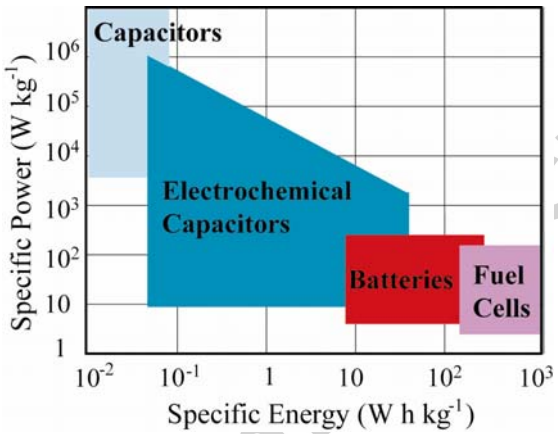

Figure 1 A simplified Ragone plot of specific power versus specific energy for the various electrochemical energy storage devices.

Among these various energy storage systems, batteries and ECs are two key technological systems that have found a broad range of applications. The basic differences between batteries and ECs lie in their different charge storage mechanisms and their materials/structures. Typically batteries are designed to provide high energy density by storing charge in bulk electrodes (bulk storage) through faradaic reactions, and they have been the technology of choice for many applications with virtually all portable electronics relying on energy stored chemically in them. However, due to physical changes in materials/structures between the charged state and the discharges state, current battery technologies have performance limitations such as short cycle life and calendar life and slow charge/discharge rates (limited power capability). In contrast, ECs are

designed to take advantage of near-surface charge storage mechanisms (based on electrochemical double-layer capacitance or redox pseudocapacitance, see Section 2) to achieve much greater power density (1-2 orders of magnitude higher than that of batteries) at some expense of their energy density. Though limited in specific energy (5-10 W h kg^{-1} for ECs versus 100~250 W h kg^{-1} for Li-ion batteries), ECs can provide the ability to store and release the energy within time frame of a few seconds, compared to tens of minutes or more needed to charge/discharge for batteries. Moreover, ECs exhibit superior cycle life that is typically measured in hundreds of thousands to millions of cycles, 2-3 orders of magnitude better than that of batteries. Last but not the least, ECs also offer high reliability and better safety versus batteries, leading to a much lower maintenance cost [4, 9].

With high power capability, exceptional cycle life and reliability, ECs have been used in a variety of applications ranging from portable consumer electronics, computer memory backup systems, to hybrid electric vehicles and all-electric vehicles, and to large industrial scale power and energy management [10-12]. The fast charge/discharge characteristics and long cycle life make ECs particularly suitable for recycling energy from repetitive motion (e.g. automotive braking, elevator operation) that would otherwise be wasted, leading to the improved energy efficiency [9]. In a hybrid power system, ECs can be combined with energy-dense, but power-limited components such as batteries and fuel cells in order to enhance the system lifetime, reduce the total system weight and volume, and increase the overall efficiency [13]. ECs can also be used for power quality applications in the industry, such as for uninterruptible power supplies (quick response from the storage bringing the grid up to full power in a matter of seconds) and load-

leveling to provide high quality power, which can greatly reduce economic losses that result from power disruptions [12].

In the past decade, EC technology has experienced an impressive growth in terms of the increase in performance owing to the discovery of new electrode materials, especially nanomaterials, and the design of new hybrid systems that combine faradaic and capacitive electrodes [10]. Given their unusual electrical, mechanical and surface properties due to confined dimensions of such materials, nanostructured materials become increasingly important for electrochemical energy storage [14, 15]. The promising advantages and associated disadvantages of nanostructured electrode materials have been discussed and reviewed previously [16]. Key advantages include short electron and ion transport path, large surface area between electrode and electrolyte, and new reactions not possible with bulk materials. Main disadvantages include increased undesirable reactions at the electrode/electrolyte interface due to high surface area and potentially more complex synthesis and higher manufacturing cost.

Although the research to improve the electrode performance of nanomaterials has dramatically increased, there are still no standardized test methods for accurately determining a material's performance for use as an EC electrode. Various techniques and experimental procedures are currently being employed leading to wide variations in reported results. Recently, Ruoff *et al.* discussed best practice methods that will enable the more accurate determination and reporting of an electrode material's performance [17]. They recommended a more standard and accurate test based on a two-electrode configuration to resemble the physical configuration and internal voltages that occur in a packaged ultracapacitor, thus providing the best indication of an electrode material's

performance. Moreover, the mass loading of the active material on the order of ~10 mg cm^{-2} and the electrode thicknesses on the order of ~15 μm (close to that of packaged commercial cells) should be implemented with the same electrolytes used in actual capacitors. It should be noted that energy density and power density are not appropriate for material level performance reporting since they strongly depend on packaging parameters (e.g. the mass of the dead components and cell architecture). To report meaningful energy and power densities, the test cells should be fabricated as full sized, packaged ECs and meanwhile calculations should be based on the mass of all components including the whole package.

In a most recent Perspective report by Gogotsi and Simon, a more consistent presentation of energy and power densities is again stressed [18]. They show that outstanding performance claimed for many new electrode materials may not necessarily be applicable to the actual EC performance when all device components are included, by giving an example based on some recent publication on graphene-based materials reporting high energy density comparable to that of batteries [19]. **Figure 2** reveals that reporting energy and power densities per weight of only active material on a Ragone plot (panel A) may not give a realistic picture of the performance that the assembled device could reach, because the weight of other device components (including current collectors, electrolyte, separator, binder, etc) also needs to be considered. In fact, the weight of active carbon material only accounts for ~30% of the total mass of the packaged commercial EC, and a factor of 3-4 is frequently used to extrapolate the energy or power density of the device from the performance of the material. Nevertheless, this extrapolation is only valid for electrodes with thicknesses and mass loading similar to

those of commercial electrodes. An electrode of the same carbon material that is 10 times thinner or lighter will further reduce energy density by three- to four-fold (see Figure 2A), with only a slight increase in power density.

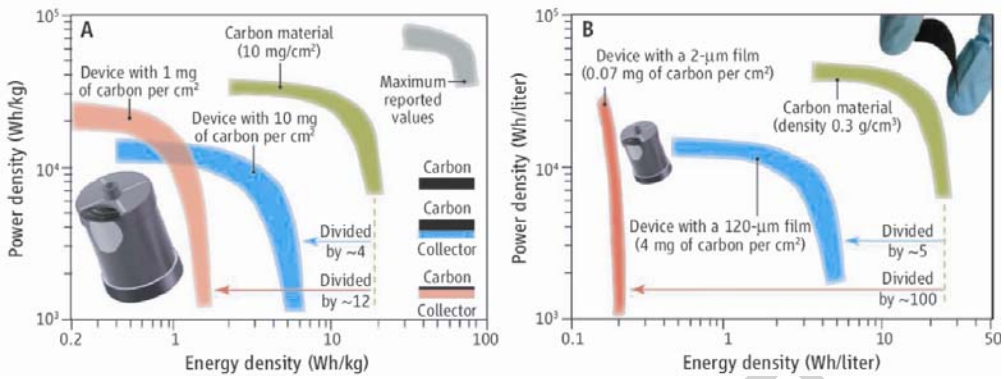

Figure 2 Two Ragone plots of power density versus energy density for the same ECs are on a gravimetric (per weight) basis in (**A**) and on a volumetric basis in (**B**). The plots show that excellent properties of carbon materials will not translate to medium- and large-scale devices if thin-film and/or low-density electrodes are used. Reproduced with permission [18]. Copyright 2011, American Association for the Advancement of Science.

When considering the energy/power density on a volumetric basis, rather than gravimetric, e.g. for a low-density graphene electrode (~0.3 g cm^{-3}) with an extremely high gravimetric energy density of 85 W h kg^{-1}, its volumetric density will be 25.5 W h L^{-1} for the electrode and ~5 W h L^{-1} for the device (see Figure 2B), which is a typical value for commercial activated carbon based ECs. Moreover, Ragone plots are only one measure of a device and they do not show other important characteristics, such as the cycle lifetime, energy efficiency, self-discharge, and others. A complete and systematic study over these parameters under standard conditions (e.g. sufficient mass loading and thickness of electrode materials, appropriate measurement conditions) is critically needed in order to present energy and power densities in a more consistent and convincing manner. This will greatly facilitate introduction of new materials and find right solutions for improving the performance of EES devices.

Energy Storage Mechanisms and Materials for Electrochemical Capacitors

Distinct from conventional electrostatic capacitors which store charges in an electric field imposed across a thin layer of dielectric material, ECs store charges at the electrochemical interfaces between the high surface area, porous electrode material and the electrolyte. The effective capacitances of ECs are typically several orders of magnitude greater than those obtained by conventional capacitors because of much larger specific surface area (500-2000 m^2 g^{-1} for ECs) and shorter distance between the electrode and electrolyte ions (in the order of nanometer, 10^{-9} m). The specific capacitance, C (F g^{-1}) of an EC can be described according to Eq. 1

$$C = \frac{\varepsilon_r \varepsilon_0 A}{d} \quad (1)$$

where ε_r is the relative electrolyte dielectric constant, ε_0 is the dielectric constant of the vacuum, d is the distance between electrolyte ions and the electrode (nanoscale charge separation distance) and A is the specific surface area of the electrodes.

Depending on the energy storage mechanisms, ECs can be classified into two general categories: electrochemical double-layer capacitors (EDLCs) and pseudocapacitors (**Figure 3)**. EDLCs, which store charges electrostatically via reversible ion absorption at the electrode/electrolyte interface (Figure 3A), commonly use carbon-based active electrode materials with high surface area [6, 20]. In contrast, pseudocapacitors use fast and reversible redox reactions at the surface of electroactive materials for charge storage (Figure 3B). The large specific pseudocapacitance of faradaic electrodes (typically 300-1000 F g^{-1}) exceeds that of carbon-based materials (typically 100-250 F g^{-1}) using double layer charge storage. Typical active pseudocapacitive materials include transition metal

oxides such as RuO_2, Fe_3O_4, NiO, and MnO_2 [21, 22], and electronically conducting redox polymers such as polyanilines, polypyrroles, and polythiophenes [23]. More details about these two energy storage mechanisms and related materials are discussed in the following.

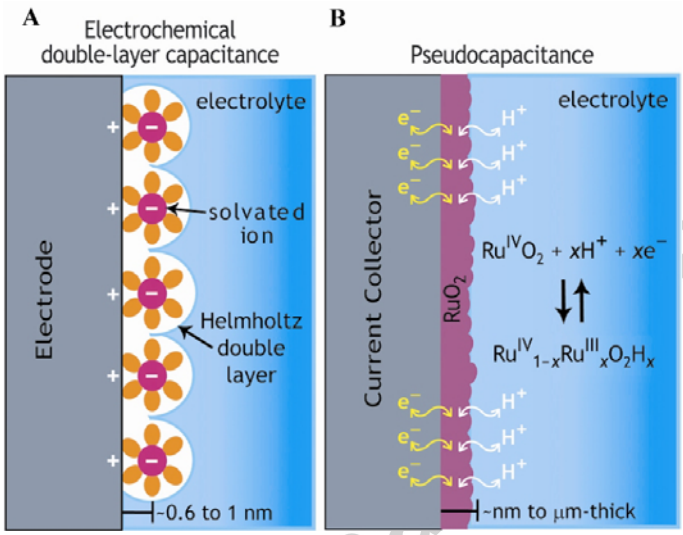

Figure 3 Schematic of two different charge storage mechanisms via (A) electrochemical double-layer capacitance (EDLC) or (B) redox reactions based pseudocapacitance. Reproduced with permission [24]. Copyright 2011, Materials Research Society.

2.1 Electrochemical Double-Layer Capacitors

Currently the most common and commercially available ECs are EDLCs where electrical energy is stored by electrostatic accumulation of charges in the electric double-layer at all electrode/electrolyte interfaces (Figure 3A). EDLCs can provide very high power and excellent cycle life due to their fast and near-surface electrochemical process. However, the energy stored in EDLCs is often limited by the finite electrical charge separation at the interface of active electrode materials and the electrolyte, and by the operating voltages that is primarily determined by the stable potential window of the electrolyte. This can be clearly seen from the following equation for the specific energy (E) of the EDLC [6, 7],

$$E = \frac{1}{2} CV^2 \quad (2)$$

where C is the cell-level specific capacitance, and V is the operating voltage of the EDLC cell. Each element is crucial to the final performance of the EDLC. The specific capacitance depends strongly on the electrode material, and can be optimized by choosing high surface area, electronically conducting materials, such as carbon-based nanomaterials [10]. On the other hand, the electrolytes need be carefully chosen and evaluated to maximize the operating voltage. Non-aqueous electrolytes with good ionic conductivity are often used for high-energy and high-power EDLCs owing to their large operational voltage window (up to 3.5 to 4 V), as opposed to a more limited potential window by aqueous-based electrolytes (generally <1.2 V). It should be noted that according to Eq. 2, a three-fold increase in voltage (V) results in nearly an order of magnitude increase in energy (E) stored at the same capacitance.

Various forms of carbon nanomaterials have been investigated and used as active materials in EDLC electrodes since these carbon-based materials offer the advantageous features including high conductivity, electrochemical stability and open porosity. Besides activated carbons (ACs) which are the most widely used active materials for EDLC applications, many other forms of nanostructured carbons, including aerogels [25], nanotubes [26, 27], carbide-derived carbons (CDCs) [28], onion-like carbons (OLCs) [29], and graphene [11, 19, 30], are being explored as alternatives to activated carbon for improving energy density while maintaining high power density in the ultimate EDLCs. Considering many recent reviews that cover more extensively on carbon-based electrode materials for ECs [31-34], herein only a few examples, which are thought to be the most recently developed and representative, are discussed below (**Figure 4**).

Gogotsi *et al.* and Simon *et al.* recently developed several unique nanostructured carbons, called carbide-derived carbons and onion-like carbons for microscale supercapacitors that have exhibited good volumetric capacity and excellent power performance, as well as high discharge rates (Figure 4A and 4B) [28,29]. Jang *et al.* reported the synthesis of curved graphene sheets for best utilization of the highest intrinsic surface capacitance (Figure 4C), and obtained graphene-based electrodes with specific energy density of 85.6 W h kg^{-1} at room temperature when using ionic liquids as electrolytes (operating at a voltage >4 V) [19]. Most recently, Ruoff and coworkers developed chemically activated graphite oxide, which is highly porous and has a surface area of up to 3100 m^2 g^{-1} (Figure 4D). The EDLC electrodes constructed with this special form of carbon yielded high values of gravimetric capacitance and energy density with organic and ionic liquid electrolytes [35].

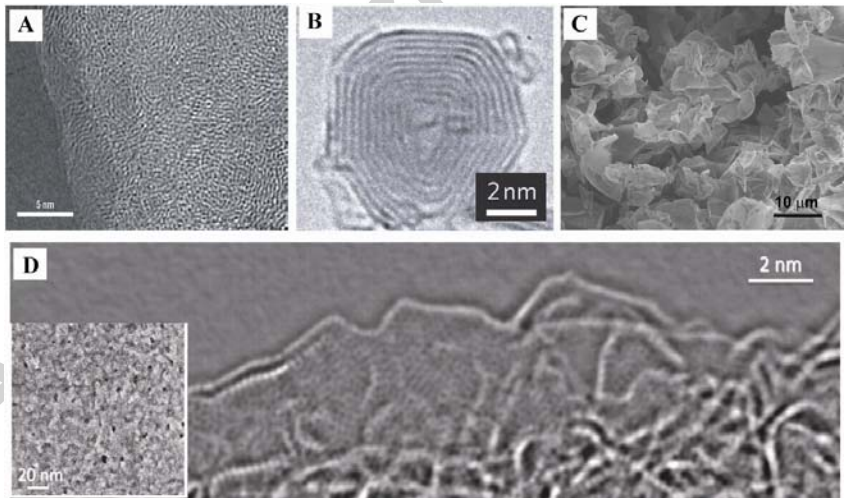

Figure 4 Carbon structures used as active materials for EDLCs. (A) Typical transmission electronic microscopy (TEM) image of a disordered microporous carbon (SiC-derived carbon). Reproduced with permission [10]. Copyright 2008, Macmillan Publishers Limited. (B) TEM image of onion-like carbon. Reproduced with permission [29]. Copyright 2010, Macmillan Publishers Limited. (C) SEM image of curved graphene sheets. Reproduced with permission [19]. Copyright 2010, American Chemical Society. (D) Reconstructed high resolution TEM image from the edge of KOH activated microwave exfoliated graphene oxide sample (a-MEGO). Reproduced with permission [35]. Copyright 2011, American Association for the Advancement of Science.

Despite these advancements made on developing new electrode materials, the ultimate specific energies of EDLCs are still fundamentally limited by their reliance on double-layer capacitance as the primary energy storage mechanism. It is difficult to further promote the performance of ECs based on pure carbon to fill the gap between batteries and ECs. Alternatively, a drastic capacitance improvement can be realized by introducing the pseudocapacitance effects through hybrid carbon with pseudocapacitance materials, as discussed in the following section.

2.2 Pseudocapacitors

In contrast to EDLCs, pseudocapacitance arises from fast and reversible electron-exchange reactions at or near the electrode surface (Figure 3B). Given the nature of the Faradaic process (redox reactions) involved in energy storage, pseudocapacitors can increase specific capacitance and energy density but at some cost of power density and cycle life when compared to EDLCs. There are two general types of pseudocapacitive materials: transition metal oxides and electronically conducting polymers. The most commonly known pseudocapacitive metal oxides include ruthenium oxide (RuO_2) [36, 37], manganese oxide (MnO_x) [22], iron oxide (Fe_3O_4) [21], nickel oxide (NiO) [38], and others. Typical electronically conducting polymers for redox pseudocapacitance are polyanilines, polythiophenes, polypyrroles, and other π-conjugated conducting polymers [23]. **Figure 5** compares the widely studied and most representative electrode materials for ECs including both carbon-based EDLC electrodes and pseudocapacitor electrodes [39].

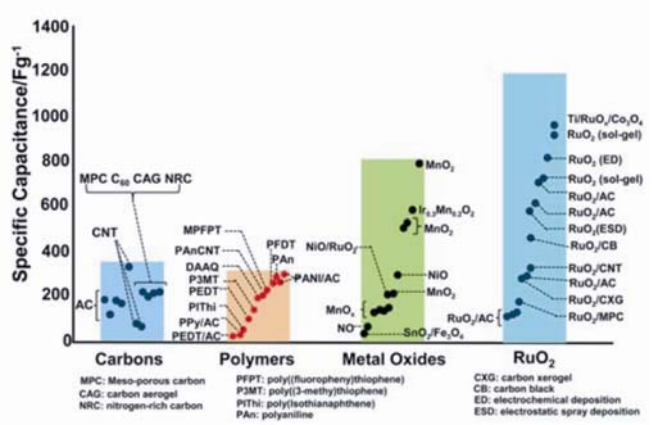

Figure 5 The capacitance performance for both carbon-based EDLC electrodes and pseudocapacitor electrodes (including transition metal oxides and conducting polymers). Reproduced with permission [19, 23, 39]. Copyright 2008, The Electrochemical Society.

RuO_2 is a widely studied pseudocapacitive material thanks to their high theoretical specific capacitance (1358 F g^{-1}) and good electronic conductivity (3×10^2 S cm^{-1}). When electrochemically cycled in acidic aqueous electrolytes, they exhibit distinct oxidation states accessible within a voltage window of ~1.2 V. The pseudocapacitive behavior of RuO_2 is generally ascribed to a series of fast and reversible electron-transfer reactions coupled with adsorption of protons on the surface of RuO_2 electrodes (see Figure 3B) where Ru oxidation states can change from (II) up to (IV), as shown in the following [10]:

$$RuO_2 + xH^+ + xe^- \leftrightarrow RuO_{2-x}(OH)_x \quad (3)$$

where $0 \le x \le 2$. The pseudocapacitive performance of RuO_2 is determined by several factors such as the degree of particle crystallinity, particle size, and electrode architecture, yielding specific psedudocapacitance of 200-1,200 F g^{-1} (Figure 5). For example, it was shown that amorphous hydrous ruthenium oxide ($RuO_2 \bullet xH_2O$) exhibited a much higher specific capacitance (720 F g^{-1}) than anhydrous ruthenium oxide [40]. Another example is that a tubular arrayed porous structure of $RuO_2 \bullet xH_2O$ electrodes yielded very high specific capacitance of ~1,300 F g^{-1} [36]. The superior electrochemical performance is

attributed to its tailored nanotubular array architecture and metallic conductivity for effective ion and electron transport, as well as its hydrous nature enabling a high rate of proton exchange. Although RuO_2 can offer excellent charge storage performance, the high cost associated with the precious metal oxide and the difficulties in large scale production limit its practical applications.

In comparison, MnO_2 is often considered the most promising transition metal oxide for pseudocapacitors due to its high theoretical specific capacitance (1370 F g^{-1}), low cost, and environmental benignity [22]. Goodenough *et al.* first reported the capacitance-like behavior for MnO_2 when electrochemically cycled in an aqueous electrolyte (2 M KCl) [41], which has catalyzed a great deal of interest in exploring MnO_2 as an active material for EC applications. The charge storage mechanism for pseudocapacitive MnO_2 is based on surface adsorption of electrolyte cations C^+ (e.g. K^+, Na^+, Li^+) as well as proton incorporation according to the reaction [10]:

$$MnO_2 + xC^+ + yH^+ + (x+y)e^- \leftrightarrow MnOOC_xH_y \quad (4)$$

However, the theoretical capacitance of MnO_2 has rarely been achieved in experiments mainly due to its poor electronic conductivity (~10^{-6} S cm^{-1}), which limits the rate capability for high power performance and thus hinder its wide applications in energy storage systems. To improve the electrical conductivity and realize high specific capacitance of MnO_2-based electrodes, considerable research efforts have been placed on exploring hybrid composite structures where MnO_2 is combined with highly conductive materials such as carbon nanomaterials and metal nanostructures. A more detailed discussion on this topic is covered in the latter part of this review.

Many kinds of conducting polymers such as polythiophene, polypyrrole, polyaniline, and their derivatives, have been investigated for EC applications as pseudocapacitive materials [42]. These π-conjugated conducting polymers with various heterocyclic organic compounds have shown high gravimetric and volumetric pseudocapacitance in various nonaqueous electrolytes with operating voltages of ~3 V. They are actively explored with expectation to enable the following properties through their molecular design: (i) devices of various and flexible shapes, (ii) light-weight devices due to their low specific gravity, and (iii) potential bio-degradability (environmentally friendly) [23]. However, when used as bulk materials, conducting polymers suffer from a limited cycling stability that leads to the decay of their electrochemical performance. Present research efforts with conducting polymers for EC applications are being directed towards hybrid electrode systems, as discussed below.

2.3 Hybrid Capacitors

In addition to EDLCs and pseudocapacitors, there is another special type of capacitor system, called 'hybrid capacitors', which usually combine one battery-type faradaic electrode (as energy source) with the other capacitive electrode (as power source) in the same EC cell [10]. In such systems, the battery-like electrode provides high energy density while the EDLC electrode enables high power capability in the system. Although this type of ECs generally shows much enhanced capacitance and greatly improved energy density compared with EDLCs [43-45], there is still a significant drawback of these hybrid capacitor devices, namely, the limited cyclability of the faradaic electrodes (considering balanced capacities for positive and negative electrodes) [39]. Numerous

combinations of positive and negative electrodes have been investigated in aqueous or organic electrolytes. Overall, the key to achieving high power and energy density hybrid ECs with long cycle life is to explore novel electrode material systems with rational design of material combination, morphology, and size, and proper choice of electrolytes that operate at high voltages and have excellent ionic conductivity and electrochemical stability. Note that this special category of ECs using two different types of materials (EDLC- and Pseudocapacitance-based) for positive and negative electrodes is different from the topic of 'hybrid nanostructured materials as high-performance electrodes for ECs' that we review in the following section.

Hybrid Nanostructured Materials as High-Performance EC Electrodes

The electrochemical performance of ECs can be achieved by introducing pseudocapacitance effects into hybrid composite electrode systems combining nanostructured carbons with pseudocapacitive materials, such as transition metal oxide and electrically conducting polymers [46]. Forming hybrid structures with highly conductive carbons is one of the most adopted methods to improve the device performance of metal oxide electrodes whose poor conductivities (*e.g* MnO_2, ~10^{-6} S cm^{-1}) limit their capacitance, cycling life and rate performance.

3.1 Hybrid Electrodes based on Carbon and Metal Oxides

3.1.1. Carbon/MnO_2 Hybrid

As one of the most promising candidates for ECs, MnO_2 has attracted much attention because of its superior electrochemical performance, low cost, and environmentally benign nature. The hybrid structures of MnO_2 and various carbon materials (such as

activated carbons, carbon aerogels, CNTs, and graphene, etc) were actively explored for EC applications in the past decade [47,48].

Carbon nanofibers were used as the base supporting materials to deposit MnO_2 forming the hybrid structures of carbon/MnO_2. Li *et al.* demonstrated hybrid supercapacitor electrodes by coaxially coating MnO_2 thin films on a vertically aligned carbon nanofiber array [49]. Ultrathin MnO_2 layers were uniformly coated via cathodic electrochemical deposition. This unique 3D brush-like vertical microstructure of carbon nanofibers/MnO_2 core-shell array provides the highly conductive and robust core and reliable electrical connection to the thin MnO_2 shell. The specific pseudocapacitance of 313 F g^{-1} in addition to the EDL capacitance of 36 F g^{-1} was achieved at a scan rate of 50 mV s^{-1} and maintained at this level as the scan rate was increased up to 2 V s^{-1}. A maximum specific capacitance of 365 F g^{-1} was demonstrated in the sample with ~7.5 nm thick MnO_2. This hybrid core-shell nanostructure demonstrates high performance with maximum specific energy (~32.5 W h kg^{-1}), specific power (~6.2 kW kg^{-1}), and cycle stability of ~11 % capacitance drop after 500 cycles. Wu *et al.* deposited needle-like manganese oxide (alpha-MnO_2) nanofibers onto the conductive carbon fiber fabric for EC application [50]. The results revealed that protons intercalated into the interior region of the MnO_2 bulk in aqueous electrolytes, whereas the alkali metal cations only reached the near−surface region. The specific capacitance of MnO_2 nanofibers coated on carbon fabric could reach as high as 432 F g^{-1}, which is much higher than that of MnO_2 nanofibers coated on stainless steel (177 F g^{-1}) at a current density of 5 A g^{-1} in 1 M Na_2SO_4 aqueous electrolyte.

Porous carbons such as carbon aerogels and mesoporous carbons were also used to produce carbon/MnO_2 hybrid structures. Tong and coworkers developed a synthesis route for preparing mesoporous MnO_2/carbon aerogel composites [51]. The deposited MnO_2 was found to have a hybrid mesoporous structure which may optimize the electronic and ionic conductivity to minimize the total resistance of the system and thereby maximize the performance characteristics of this material for use as EC electrodes. In this hybrid, high specific capacitance (515.5 F g^{-1}) was demonstrated, showing the potential of mesoporous MnO_2/carbon hybrid as a high-performance electrode material. Lu *et al.* prepared carbon aerogel/Mn_3O_4 composite electrodes by a self-limiting anodic electrochemical deposition of manganese oxide [52]. Mn_3O_4 was grown in the form of thin nanofibers along the backbone of the carbon aerogel as shown in **Figure 6A** and **6B**, leaving adequate space for the electrolyte and enabling a fuller extent of the utilization of the Mn_3O_4. At a scan rate of 25 mV s^{-1}, the specific capacitance of the hybrid electrode reached a maximum value of 503 F g^{-1} and experienced only a small decay of ~1% at the 6000th cycle. The power density reached 48.5 kW kg^{-1} with energy density of 21.6 W h kg^{-1} at a scan rate of 500 mV s^{-1}. Lu *et al.* synthesized mesoporous carbon/MnO_2 hybrid structures with hierarchical pore structures and controllable MnO_2 loading using a self-limiting growth method [53]. The reaction was carried out by using redox reactions of $KMnO_4$ with sacrificed carbon substrates that contain hierarchical pores. The unique pore structure allows the synthesis of hybrid nanostructures with tunable MnO_2 loading up to 83 wt%. The carbon/MnO_2 hybrid electrode with 70 wt % MnO_2 content, showed a specific capacitance of 218 F g^{-1} at 0.1 A g^{-1} and good capacitance retention of 70 % at 2 A g^{-1}.

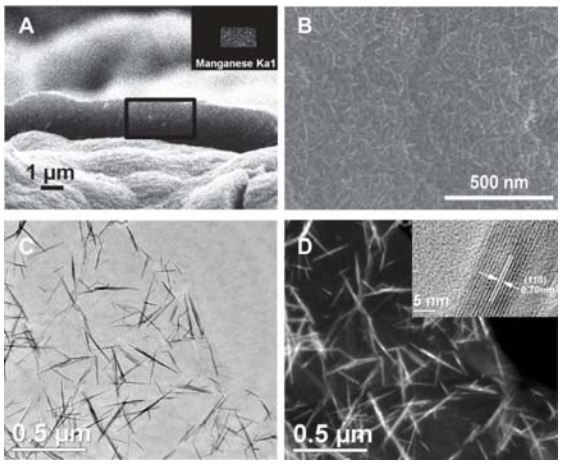

Figure 6 SEM and TEM images of carbon aerogel/Mn_3O_4 (A-B) and graphene oxide (GO)/MnO_2 hybrid structures (C-D). (A) Cross-sectional SEM image of carbon aerogel/Mn_3O_4 hybrid. Inset is the area-scan elemental analysis for Mn across the composite layer. (B) Top-view SEM image of carbon/Mn_3O_4 aerogel hybrid. Reproduced with permission [52]. Copyright 2011, Wiley VCH. (C) Bright-field TEM image of GO/MnO_2 hybrid. (D) Dark-field TEM image of GO/MnO_2 structure and the HRTEM image of a MnO_2 nanoneedle (inset). Reproduced with permission [54]. Copyright 2010, American Chemical Society.

Besides amorphous carbons, MnO_2 hybrid materials with CNTs and graphene (or graphene oxides) were also intensively studied in recent years. Gu and coworkers prepared MnO_2 nanoflower/carbon nanotube array (CNTA) hybrid electrodes with hierarchical porous structure, large surface area, and good conductivity. The hybrid structure was prepared by electrodepositing technique on the vertically aligned CNTA framework [55]. This binder-free MnO_2/CNTA electrode exhibited good rate capability (~50% capacity retention at 77 A g^{-1}), high capacitance (199 F g^{-1} and 305 F cm^{-3}), and long cycle life (3% capacity loss after 20,000 charge/discharge cycles). Yang *et al.* deposited MWCNTs/MnO_2 hybrid based thin film electrodes via the layer-by-layer (LbL) assembly method [56]. These LbL assembled CNTs/MnO_2 thin films consisted of a uniform coating of nanosize MnO_2 on the CNT network. Hybrid CNTs/MnO_2 electrodes yielded a significantly higher volumetric capacitance of 246 F cm^{-3} with good capacity

retention up to 1000 mV s^{-1} thanks to rapid electron and ion transport within the electrodes. Lee *et al.* electrodeposited MnOx nanoparticles onto CNT sheets [57]. The CNT sheets were prepared by drawing directly from MWCNT forests, in which the MWCNTs are aligned in the drawing direction, providing well-ordered conductive paths. Flower-shaped MnOx particles were electrochemically deposited directly on CNTs, ensuring good electrical contacts between MnOx particles and the CNTs. The resulting hybrid materials showed specific capacitance of ~510 F g^{-1}. Zhu *et al.* synthesized a hybrid structure based on needle−like MnO_2 nanocrystals supported by graphene oxide (GO/MnO_2 hybrid), as shown in Figure 6C and 6D [54]. The hybrid was prepared by a simple soft chemical route in a water-isopropyl alcohol system. They proposed a microstructure formation mechanism as intercalation and adsorption of Mn ions into GO sheets, followed by the nucleation and growth of the crystal species via dissolution-crystallization and oriented attachment, which in turn results in the exfoliation of GO sheets. A synergistic effect by the interaction between GO and MnO_2 was found to enhance the electrochemical performance of as-prepared hybrid electrodes. The GO/MnO_2 hybrid electrodes (~84 % capacitance retention from 197.2 F g^{-1} to 165.9 F g^{-1}) shows improved electrochemical stability than that of MnO_2-only sample (69 % retention from 211.2 F g^{-1} to 145.7 F g^{-1}) after 1,000 cycles at current density of 200 mA g^{-1}. Similarly, Zhao *et al.* prepared hybrid materials of reduced graphene oxide (RGO) and MnO_2 [58]. Functionalized graphene was prepared by reducing graphene oxide with poly(diallyldimethylammonium chloride) (PDDA), changing the surface charge from negative to positive. The MnO_2 nanosheets were then dispersed on functionalized RGO sheets. The hybrid material exhibited enhanced capacitive performances than those of

pure functionalized RGO and Na-typed birnessite (Na/MnO_2) sheets. The hybrid material showed good cycle stability with over 89% of original capacitance was retained after 1,000 cycles.

3.1.2. Carbon/RuO_2 Hybrid

The RuO_2/CNTs hybrid structures were investigated by several research groups. For example, Sheu and coworkers demonstrated a novel type of RuO_2/MWCNTs hybrid electrode for supercapacitors [59]. The hybrid structure was formed by magnetic sputtering Ru onto MWCNTs in Ar/O_2 atmosphere, which were synthesized on Ta plates by chemical vapor deposition. TEM and SEM characterizations revealed that the RuO_2 film on the surface of the CNTs was composed of small crystalline grains with tilted bundle-like microstructures. The capacitance of the electrodes was significantly increased from 0.35 to 16.94 mF cm^{-2} by modification with RuO_2, indicating the enhanced capacitance by additional pseudocapacitive RuO_2. Ramaprabhu *et al.* synthesized a series of hybrid materials of CNTs/RuO_2, CNTs/TiO_2, and CNTs/SnO_2 for supercapacitor electrodes via a chemical reduction method using functionalized CNTs and respective salts [60]. Specific capacitances of RuO_2, TiO_2, and SnO_2 dispersed MWNT electrodes are significantly increased compared to that of pure MWNT electrodes owing to the pseudocapacitance of the nanocrystalline metal oxides dispersed on the functionalized MWNTs.

3.1.3. Hybrid Carbon and Other Metal Oxides

Vanadium pentoxide (V_2O_5) layered nanostructures are known to have very stable crystal structures and high faradaic activity. However, V_2O_5 has low electronic conductivity. Forming hybrid structures with conductive carbons can improve the ECs performance of V_2O_5. Lee *et al.* electrodeposited an ultrathin V_2O_5 layer on a self-standing carbon nanofiber paper [61]. A high specific capacitance of 1308 F g^{-1} was obtained in a 2 M KCl electrolyte when normalized to only vanadium oxide (~3 nm thickness), which contributed to over 90% of the total capacitance (214 F g^{-1}) despite the low weight percentage of the V_2O_5 (15 wt %). The high capacitance of the V_2O_5 is attributed to the large external surface area of the carbon nanofibers and the maximized active sites for redox reactions of the ultrathin V_2O_5 layer. Fang *et al.* studied the capacitive properties of hybrid V_2O_5/CNTs material [62], which were prepared by coating an uniform V_2O_5 thin film on CNT arrays. The V_2O_5/CNTs hybrid showed significantly improved capacitive performance, as compared with that of bare V_2O_5 films or pristine CNTs.

The hybrid structures between nanostructured carbons and other metal oxides such as NiO and Co_3O_4 were all found capable of enhancing EC performance. Dai and coworkers synthesized single crystalline $Ni(OH)_2$ hexagonal nanoplates grown on graphene sheets with various degrees of oxidation (**Figure 7A** and **7B**) as supercapacitor electrode materials [63]. The hybrid nanostructured material exhibited a high specific capacitance of ~1,335 F g^{-1} at a charge/discharge current density of 2.8 A g^{-1} and ~953 F g^{-1} at 45.7 A g^{-1}. As a control, a simple physical mixture of pre-synthesized $Ni(OH)_2$ nanoplates and graphene sheets showed lower specific capacitance, highlighting the importance of

interface between $Ni(OH)_2$ nanoplates and graphene sheets. Single-crystalline $Ni(OH)_2$ nanoplates directly grown on graphene sheets also significantly outperform small $Ni(OH)_2$ nanoparticles grown on heavily oxidized, electrically insulating graphite oxide (GO), suggesting that the electrochemical performance of these composites is dependent on the quality of graphene substrates and the morphology and crystallinity of metal oxide nanomaterials grown on top.

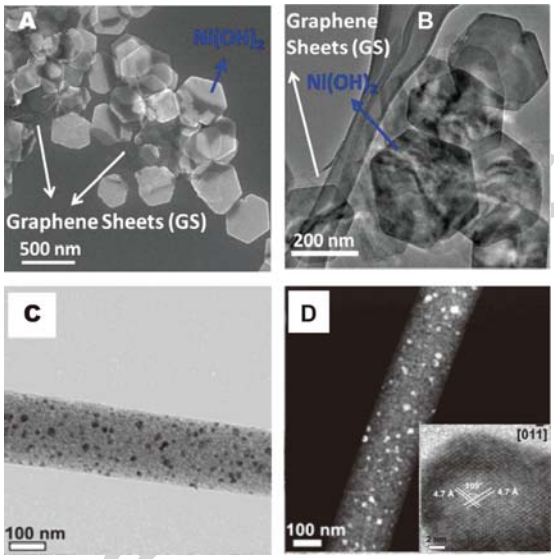

Figure 7 SEM and TEM images of graphene/$Ni(OH)_2$ hybrid structures (A-B) and nanoporous carbon/Co_3O_4 hybrid (C-D). (A) SEM image of $Ni(OH)_2$ nanoplates grown on graphene sheets (GS). (B) TEM image showing $Ni(OH)_2$ nanoplates grown on GS. Reproduced with permission [63], Copyright 2010, American Chemical Society. TEM (C) and dark-field STEM (D) images of nanoporous carbon/Co_3O_4 hybrid structures. Inset is the HRTEM image of a Co_3O_4 nanocrystal. Reproduced with permission [64]. Copyright 2010, American Chemical Society.

Mullen and coworkers reported an *in situ* fabrication of hybrid structures of Co_3O_4 nanocrystals and 1D nanoporous carbons (NPCs) (Figure 7C and 7D) via an organometallic precursor-controlled thermolysis approach [64], and found that the integration of metallic nanocrystals and electronically conducting carbons to form metal−carbon hybrids can lead to much enhanced physical and chemical properties. The synthesis involves impregnating 3,4−bis(4−dodecynylphenyl)−substituted

cyclopentadienone and its relevant cobalt into the nanochannels of anodic alumina oxide (AAO) membranes, followed by subsequent thermolysis to transform the polyphenylene backbones into 1D nanoporous carbonaceous framework. After removal of the AAO template, NPCs/Co_3O_4 hybrid was obtained, with high quality Co_3O_4 nanocrystals distributed homogeneously within the carbon framework. NPCs/Co_3O_4 was evaluated as an electrode material in a supercapacitor, for which Co_3O_4 nanocrystals contributed an exceptionally high gravimetric capacitance of ~1,066 F g^{-1}.

3.2 Hybrid Electrodes based on Carbon and Conducting Polymers

Conducting polymers such as polyaniline (PAni), polypyrrole (PPy), and polythiophene, have been extensively investigated as active electrode material in energy storage systems in the past two decades [23, 65]. They are unique electroactive materials with large π− conjugation length and reversible redox and doping/dedoping reactions. However, conducting polymers have the shortcomings of poor cycle life (only a few thousand cycles) and fast decayed capacitance in high rate cycling process, presumably due to significant volume changes during the capacitor operation and the accompanied decrease of their electrical conductivity. Moreover, the dopants may affect the chemical stability, hence the cycling stability of the conducting polymers.

The hybrid materials of carbon and conducting polymers show synergistic effects that combine the advantages of both materials. Conducting polymers provide superior pseudocapacitance, while nanostructured carbon materials act as a framework that helps conducting polymers to sustain from the strains in charging/discharging cycling process. Currently, the research in this field is focused on tuning the micro-/nano- structure of the

hybrid material, improving the interface between carbons and conducting polymers, and controlling the chemical structure of conducting polymer for high electrochemical activities. Moreover, the studies on hybrid materials of conducting polymers and carbons with different chemical compositions, morphology, and phase structure are crucial for fundamental understanding of the interface between carbons and conducting polymers, which in turn provides the basis for future improvements of their device performance.

3.2.1. Hybrid Microstructured Carbons/Conducting Polymers

Carbons of various forms of microstructures (CNTs and graphene are discussed separately in different sub-sections) have been used to form hybrid structures with conducting polymers for EC applications, for example, activated carbon (AC), and other nanostructured carbons. This field has been actively explored in the past decade given a wide range of morphologies and phase structures of carbon materials.

The AC/conducting polymer hybrid offers the advantages of moderate cost and promising scalability for mass production together with high EC performance. Morallón *et al.* compared the electrochemical performance of AC/PAni hybrids prepared by different electrochemical methods [66]. It is found that specific capacitances of all the hybrids were higher than the sum of that of the individual components. Moreover, the synthesis conditions strongly affected the electrochemical behavior of the samples. The lower the polymerization rate, the better the quality of PAni due to increased electron delocalization along the polymer chain and less branched molecular structures in the slower polymerization.

Other amorphous carbon nanostructures were also used to produce the hybrid with conducting polymers, such as carbon nanofibers (CNFs) and carbon hollow spheres. Jang *et al.* prepared PAni coated nanofibers by vapor deposition polymerization technique [67]. The CNFs with diameter of 50 nm fabricated by iron catalyzed CVD were soaked with the initiator solution, and then exposed to aniline vapor. PAni thin film was coated homogeneously on the CNFs. The coating of PAni film improved the capacitance of the CNFs, and a maximum capacitance of 264 F g^{-1} was obtained when the thickness of PAni layer was 20 nm. Yan *et al.* fabricated CNF-polyaniline composite based flexible paper for supercapacitors [68]. They electrospun polyacrylonitride into nanofibers, and turned them into carbon paper by pyrolysis. PAni/carbon hybrid paper was prepared by solution polymerization of PAni on its surface (**Figure 8A** and **8B**). The PAni/carbon hybrid paper showed a higher capacitance (638 F g^{-1} at 2 A g^{-1}) than that of pure carbon paper (317 F g^{-1}). The specific capacitance of hybrid paper remained above 90 % after 1,000 cycles. Zhao *et al.* coated PAni on hollow carbon spheres [69]. The hybrid material of PAni and hollow carbon sphere (65 wt% PAni loading) showed improved specific capacitance of 525 F g^{-1} at a current density of 0.1 A g^{-1} as compared with that of pristine hollow carbon sphere (268 F g^{-1}). This group also prepared carbon/PAni electrode materials by depositing a thin layer of PAni on the surface of 3D ordered macroporous carbons, which have a continuous carbon framework [70]. An overall capacitance of 352 F g^{-1} was obtained for the composite electrode at a current density of 0.5 A g^{-1}, which corresponded to a specific energy density of 49 W h kg^{-1}. Yushin *et al.* found that hybrid structures of PAni and detonation nanodiamond showed greatly enhanced performance as compared with that of pure PAni [71]. The cycling stability was dramatically improved,

and specific capacitance and rate capability were also increased. It was proposed that the detonation nanodiamonds embedded in PAni serve as a toughening agent of PAni, thereby minimizing the volume changes within the PAni particles during cycling and improving electrode durability of PAni-based ECs.

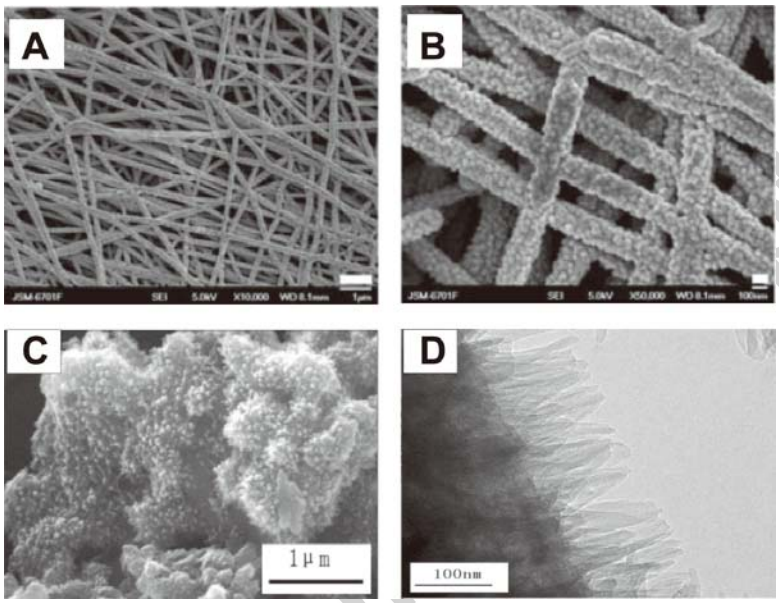

Figure 8 (A) SEM image of the carbon nanofibers/PAni hybrid paper, (B) Magnified SEM image. Reproduced with permission [68]. Copyright 2011, The Royal Society of Chemistry. (C) SEM image of mesoporous carbon/PAni hybrid, (D) TEM image of mesoporous carbon/PAni hybrid structure. Reproduced with permission [72]. Copyright 2006, Wiley VCH.

Free standing carbon micro-/nano- structures, including macroporous carbon and monolithic carbon cloth were shown to be a good 3D conducting framework as both a current collector and a high surface support for conducting polymers. One of the advantages of this type of hybrid materials is that it does not require any binder or conductive agent (e.g., PVDF or carbon black) during preparation of the electrodes. Maier *et al.* electrodeposited PAni onto a hierarchically porous carbon monolith (prepared by pyrolysis mesophase pitch against a silica monolith) [73]. A specific capacitance value as high as 2200 F g^{-1} (considering the mass of only PAni) was obtained

at a power density of 0.47 kW kg^{-1} and an energy density of 300 W h kg^{-1}. Chen *et al.* deposited PAni nanofibers on the surface of carbon cloth by two-step electrochemical polymerization of aniline [74]. This flexible supercapacitor based on PAni nanowires/carbon cloth exhibited both high gravimetric and areal capacitance. The authors obtained high gravimetric capacitance of 1,079 F g^{-1} at a specific energy of 100.9 W h kg^{-1} and a specific power of 12.1 kW kg^{-1}. Moreover, this hybrid EC electrode offered a high area-normalized capacitance of 1.8 F cm^{-2}. Such a PAni/carbon cloth hybrid shows the promise for large scale production and low cost.

Wang *et al.* prepared the CMK-3/PAni hybrid nanomaterials, with ordered PAni nanofibers grown on the surface of ordered mesoporous carbons (OMC) as shown in Figure 8C and 8D [72]. The hybrid material exhibited a high specific capacitance of 900 F g^{-1} at charge–discharge current density of 0.5 A g^{-1}. It should be noted that the capacitance value is even higher than that of amorphous hydrated RuO_2 (840 F g^{-1}), indicating that this hybrid material of carbon and conducting polymer could be a potential candidate for high performance ECs to replace rare metal oxide RuO_2. Moreover, the capacitance retention of the hybrid was about 85% when the charge−discharge current density increased 10 times from 0.5 A g^{-1} to 5 A g^{-1}. The capacitance remained ~95% after 3000 cycles. Song *et al.* did a systematic study to compare the EC performance of four samples [75]: 1) PAni fully filled OMC (50 wt % PAni loading); 2) PAni coated OMC with its mesopores remained (PAni, 50 wt %) (PAni only coated outside the OMC but not inside the mesopores); 3) physical blend of PAni and OMC (PAni, 50 wt %); and 4) pure OMC. It is found that the capacitance of PAni fully filled OMC (hybrid 1) (747 F g^{-1}) and PAni coated OMC (hybrid 2) (694 F g^{-1}) were greatly larger than the simple

physical blend of PAni and OMC (336 F g^{-1}) at a current density of 0.1 A g^{-1}, indicating a synergetic effect that the hybrid structure of OMC/PAni can increase the supercapacitor performance. Hybrid 1 showed much better EC performance than hybrid 2 at high current densities. At a current density of 3 A g^{-1} the specific capacitance of hybrid 1 was still ~492 F g^{-1}, which is about 66 % of the specific capacitance at a current density of 0.1A g^{-1}, while that of hybrid 2 was only about 40 %. This indicated that fully contact interface between OMC and PAni of the hybrid 1 improved charge transport, thus improving the efficiency of faradaic charge transfer. Meanwhile, the OMC framework was favorable for PAni to resist the large volume change during the charge/discharge cycles.

3.2.2. Hybrid CNTs/Conducting Polymers

Hybrid structures of CNTs and conducting polymers were extensively researched with the expectation that the high conductivity and high specific surface area of CNTs can greatly enhance the ECs performance of conducting polymers. Hammond and coworkers deposited hybrid thin film electrodes of PAni nanofibers and functionalized MWCNTs by LbL assembly for electrochemical capacitors (**Figure 9A** and **9B**) [76]. Highly stable cationic PAni nanofibers, synthesized from the rapid aqueous phase polymerization of aniline, were assembled with carboxylic acid (-COOH) functionalized CNTs into LbL films. The LbL-PAni/CNTs hybrid consists of a nanoscale interpenetrating network structure with well-developed nanopores that yield good electrochemical performance for energy storage applications. These LbL-PAni/CNTs films in lithium cell can store high volumetric capacitance (~238 F cm^{-3}) and high volumetric capacity (~210 mA h cm^{-3}). In addition, rate dependent galvanostatic tests showed that LbL-PAni/CNTs hybrid

structures can deliver both high power and high energy density (~220 W h L^{-1} and ~100 kW L^{-1}) and could be a good positive electrode material for thin film microbatteries or ECs.

Gao *et al.* synthesized PAni/SWCNT hybrid films through an *in situ* electrochemical polymerization/degradation process [77]. Cyclic voltammetry (CV) tests revealed good electrochemical properties of the free-standing PAni/SWCNT hybrid films. PAni/SWCNT hybrid films with 90 electrochemical polymerization cycles showed the highest specific capacitance of 501.8 F g^{-1}. And this value reached 706.7 F g^{-1} after the electro-degradation process, an improvement of ~40%, which was attributed to more available charge transfer channels and increased polycrystalline PAni regions that were produced by the dissolution of off-lying disordered PAni. Chen and coworkers demonstrated transparent and flexible supercapacitors assembled from PAni/SWCNT hybrid thin film electrodes [78]. The ultrathin, optically homogeneous and transparent, electrically conducting films of the PAni/SWCNT hybrid showed a large specific capacitance due to combined electrochemical double layer capacitance and pseudocapacitance mechanisms. A supercapacitor cell assembled using these electrodes with a SWCNT density of 10.0 mg cm^{-2} and 59 wt% PAni yielded a specific capacitance of 55 F g^{-1} at a current density of 2.6 A g^{-1}, showing its potential for transparent and flexible energy storage.

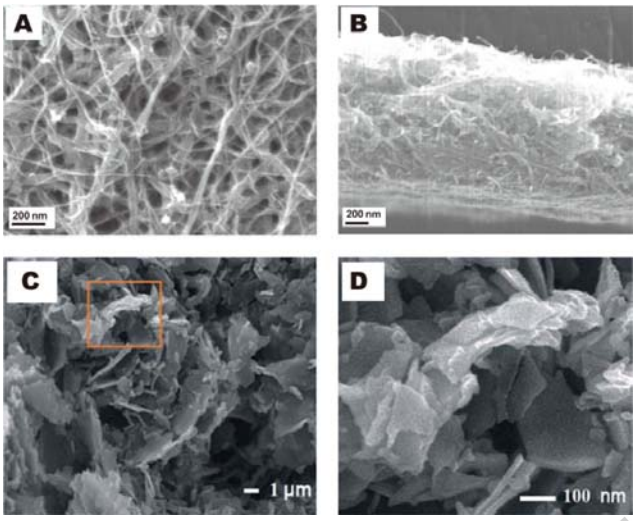

Figure 9 (A) SEM image of LbL-PAni/CNTs hybrid thin film. (B) Cross-section SEM image of the LbL film. Reproduced with permission [76]. Copyright 2011, American Chemical Society. (C) SEM image of PAni/graphene hybrid structure. (D) Magnified SEM image of (C). Reproduced with permission [79]. Copyright 2011, The Royal Society of Chemistry.

3.2.3. Hybrid Graphene/Conducting Polymers Hybrid

Graphene/conducting polymer hybrid materials have received considerable attention and present one of the most promising directions for high-performance hybrid EC electrodes [80]. Cheng *et al.* studied the supercapacitor performance of *in situ* polymerized PAni on carbon blacks, CNTs, and graphene nanosheets [81]. It was found that among all these hybrid structures, PAni/graphene hybrid showed the lowest internal resistance, the largest specific capacitance, as well as the highest cycling stability and rate capability, because of the high conductivity of graphene, improved interfacial contact of graphene/PAni due to the planar morphology of graphene, and therefore the stability to sustain the strain induced in the charge/discharge process.

Huang and coworkers described a novel one-step electrochemical co-deposition synthesis of graphene/PAni hybrid films using graphite oxide and aniline as the starting

materials [82]. The graphene/PAni hybrid film showed large specific surface area, high conductivity, and fast redox properties. The hybrid structure of graphene/PAni also showed the potential as high performance supercapacitor electrode, with a high specific capacitance of 640 F g^{-1} and good cycling stability of 90% capacitance retention after 1,000 cycles. Shi *et al.* produced PAni nanosheets by electropolymerization of aniline monomer in the aqueous electrolyte containing sulfonated-PAni-functionalized graphenes (SPAni-Gs) [79]. The as-prepared nanosheets have a thickness of ~10 nm. The resultant samples have a loosely stacked morphology on the surface of electrodes, giving a large effective surface area accessible to the electrolyte (Figure 9C and 9D). The PAni nanosheets had a large specific capacitance of 372 F g^{-1} at a current density of 0.3 A g^{-1}, ~5× higher than that of a normal PAni film synthesized in the absence of SPAni-Gs. Yu and coworkers developed flexible, uniform graphene/polypyrrole composite films using a pulsed electropolymerization technique for supercapacitor electrodes [83]. A specific capacitance as high as 237 F g^{-1} was obtained for a total deposition time of ~120 s, which is approximately four times higher than the specific capacitance of initial graphene film. This flexible supercapacitor film exhibited high energy and power densities with values of ~33 W h kg^{-1} and ~1,184 W kg^{-1}, respectively, at a scan rate of 10 mV s^{-1}.

3.3 Hybrid Ternary Electrodes based on Carbon/Metal Oxides/Conducting Polymers

In addition to binary hybrids that have been explored to improve the electrochemical performance of conducting polymers and metal-oxides, ternary hybrid structures have been recently explored as a new design that could combine the advantages from all

components: conducting carbon, and pseudocapacitive metal oxides and conducting polymers [84]. By taking advantage of the synergistic effects from the ternary hybrid, it is possible to effectively utilize the full potential of all the desired functions of each component. Thus, this ternary hybrid structure provides a direction toward solving the potential problems and is promising for the next generation high-performance electrochemical electrodes.

Liu and coworkers designed a ternary hybrid material composed of metal oxide (MnO_2), carbon nanotube (CNT), and conducting polymer (CP) [85] (Figure 10A-C). Each component in the MnO_2/CNT/CP film provides the unique and critical function to achieve the optimized electrochemical properties. CNTs not only provide high surface for the deposition of hierarchical MnO_2 porous nanospheres, but also improve the electrical conductivity and the mechanical stability of the composite; PEDOT-PSS functions as an effective dispersant for MnO_2/CNTs structures, as well as a binder material that improves the adhesion to the substrate and the connection among MnO_2/CNTs particles in the film; and the highly porous MnO_2 nanospheres provide high surface area for improved specific capacitances. Working together, these components assemble into a mesoporous, interpenetrating network structure, which offers the composite with high specific capacitance, excellent rate capability, and long cycling life stability. Specific capacitance of the ternary composite electrode reached 427 F g^{-1}. Even at high mass loading and high concentration of MnO_2 (60%), the film still showed specific capacitance value of ~200 F g^{-1}. The hybrid electrode also exhibited excellent charge/discharge rate and good cycling stability, retaining over 99% of its initial charge after 1,000 cycles.

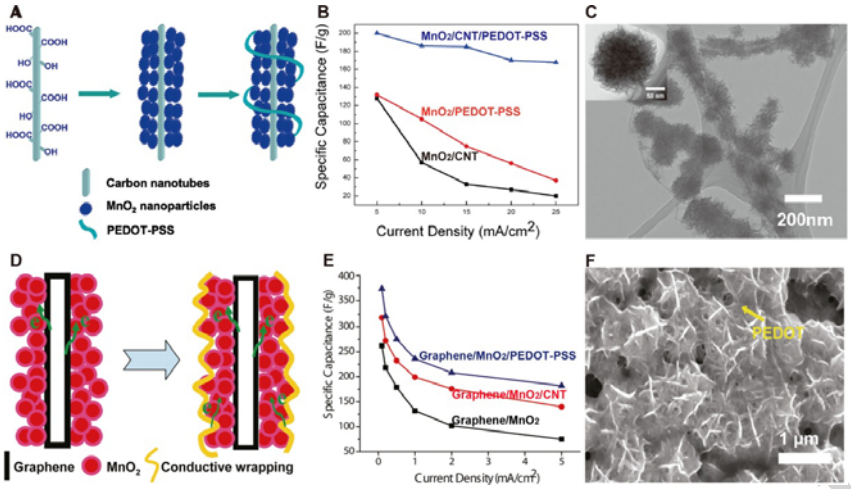

Figure 10 (A-C) Ternary hybrid structures of MnO_2/CNTs/PEDOT-PSS, (D-F) Ternary hybrid structures of graphene/MnO_2/PEDOT-PSS. (A) Schematic of MnO_2/CNTs/PEDOT-PSS ternary composite material, (B) Specific capacitance of MnO_2/CNTs/PEDOT-PSS ternary composite (blue), MnO_2/PEDOT-PSS composite (red), and MnO_2 film (black) at different charge/discharge current densities, (C) TEM of PEDOT-PSS dispersed MnO_2 nanospheres *in situ* grown on CNTs. Reproduced with permission [85]. Copyright 2010, American Chemical Society. (D) Schematic illustration showing the conductive wrapping of graphene/MnO_2 (GM) to introduce an additional electron transport path, (E) Summary plot of specific capacitance values for three different electrode systems: GM-, GMC-, and GMP-based textiles at various current densities. (F) Typical SEM image showing graphene/MnO_2/PEDOT:PSS nanostructures (GMP). Reproduced with permission [86]. Copyright 2011, American Chemical Society.

Yu and coworkers developed a "3D conductive wrapping" method to greatly improve the supercapacitor performance of graphene/MnO_2-based nanostructured electrodes [86] (Figure 10D-F). By 3D conductive wrapping of graphene/MnO_2 nanostructures with CNTs or conducting polymers, specific capacitance of the electrodes (considering total mass of active materials) has substantially increased by ~20% and ~45%, respectively, with values as high as ~380 F g^{-1} achieved. Moreover, these ternary composite electrodes have also exhibited excellent cycling performance with >95% capacitance retention over 3,000 cycles. This 3D conductive wrapping approach presents a general direction for enhancing the device performance of metal oxide-based electrochemical supercapacitors and can be generalized for designing next-generation high-performance energy storage

devices. Moreover this work shows the introduction of additional conductive materials (CNTs or CPs) by a simple dipping technique can enhance the overall electrochemical performance of hybrid electrodes.

These novel ternary hybrid systems take advantages of the synergistic effects from the hybrid structures, and make possible to effectively utilize the full potential of all the desired functions of each component. The new ternary hybrid system shows the advantages of high loading of active materials, excellent power and energy density, long cycling life, and provides a new perspective for designing electrode architectures for next generation high-performance ECs.

Novel Support Structures for Loading Hybrid Nanomaterials

ECs prepared from pseudocapacitive transition-metal oxides are predicted to have a high capacitance while also being inexpensive and environmentally friendly [22]. However, as discussed above, most pseudocapacitive transition-metal oxides have poor electrical conductivity, such as MnO_2 with a conductance of 10^{-5}-10^{-6} S cm^{-1}. In addition, the surface redox reactions, from which the pseudocapacitance comes, only happen within a very thin layer of the active materials. Great effort has been made to fabricate nanostructured pseudocapacitive materials aiming to enlarge the specific surface area and shorten the electron conduction length [87-90]. Another approach is loading pseudocapacitive materials onto conductive and porous supports with large specific surface area. Lang *et al.* reported an EC prepared by depositing MnO_2 onto a nanoporous gold substrate (**Figure 11**) which promotes electron transport and facilitates fast ion diffusion between the MnO_2 and the electrolytes, achieving a high specific capacitance of

~1,145 F g^{-1} for MnO_2 [91]. Templated ordered mesoporous carbon has also been investigated as a conductive support for RuO_2 and MnO_2, revealing high capacitance [92, 93]. However, those well-designed supports are too expensive for large scale practical applications. Therefore, in this review, we focused on relatively low-cost carbon-based porous electrodes and novel composite electrodes fabricated by coating porous substrates, such as paper, textile, and sponge, with a thin conducting layer, which further serve as supporting substrates for controlled loading of pseudocapacitive materials.

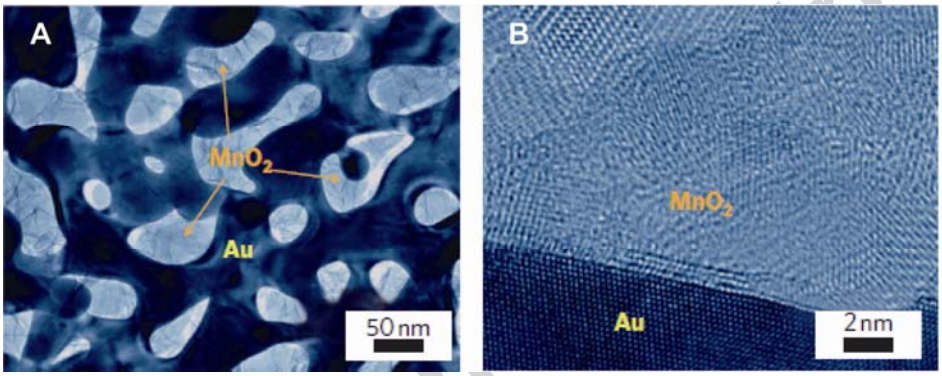

Figure 11 TEM images of nanoporous gold/MnO_2 hybrid (A-B). (A) Bright-field TEM image of the nanoporous gold/MnO_2 hybrid with a MnO_2 plating time of 20 min. The hybrid nanostructure can be identified by the contrast between the bright MnO_2 filler and the dark gold skeleton. Reproduced with permission [91]. Copyright 2011, Nature Publishing Group.

4.1 Carbon Paper and Carbon Nanofoam

Carbon paper, or carbon cloth, is a network of graphite fibers with diameters normally about several micrometers, as shown in **Figure 12A**. Due to its high porosity, large surface area, and good conductivity, carbon paper has been studied extensively as electrode materials or supporting substrate for active materials in fuel cells, batteries, and ECs [94-96]. Yang *et al.* reported hybrid EC electrodes prepared from carbon paper loaded with Co_3O_4 nanomaterials [97]. The Co_3O_4 deposited on the graphite fiber surface,

forming a secondary network consisting of nanowires with diameters of a few tens of nanometers Figure 12B. Figure 12C shows specific capacitances of the carbon paper-supported Co_3O_4 nanonet electrodes at different current densities. With a Co_3O_4 loading of 0.4 mg cm^{-2}, the highest specific capacitance achieved was 1,190 F g^{-1} at a current density of 0.25 A g^{-1}. The specific capacitance retained as high as 1,124 F g^{-1} even when the current density increased to 25.34 A g^{-1} (Figure 12C). Good rate capability was possibly due to the effective hierarchical structure design, which facilitated electron/ion transport and the redox reaction. With higher Co_3O_4 loadings of to 0.7 and 1.4 mg cm^{-2}, the composite materials still exhibited high specific capacitances of ~1,011 F g^{-1} and ~948 F g^{-1} at a current density of 14.06 A g^{-1}, respectively, and excellent rate capability. Over a 5000 cycle long term charge/discharge test conducted at a scan rate of 50 mV s^{-1}, the carbon paper supported Co_3O_4 composite showed negligible capacitance loss. The nanoscale network structure of the Co_3O_4 was claimed to be effective to release the stress caused by the volume change associated with reversible intercalation and/or adsorption of charge carrier. As a control, Co_3O_4 in the form of nanocubes was also deposited on the carbon paper, but the performance of the resulting composite was not as good as the carbon paper with Co_3O_4 nanowires (Figure 12C).

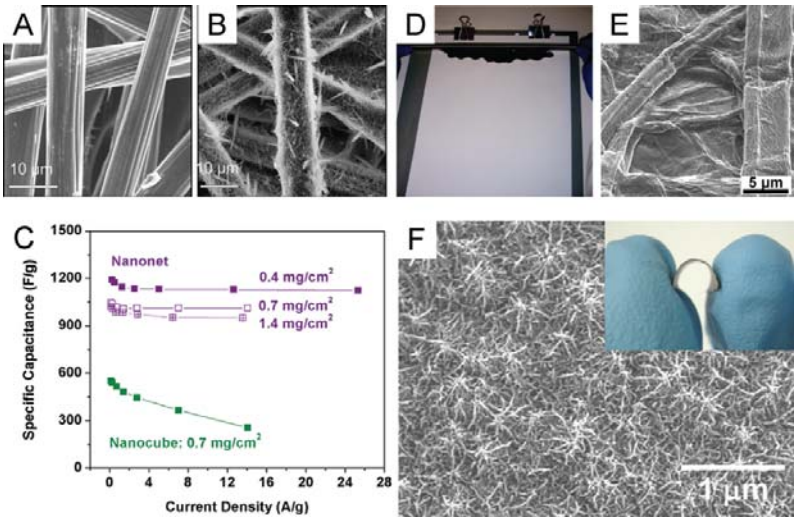

Figure 12 (A) SEM image of plain carbon paper showing 3D network structures. (B) SEM image of carbon paper with conformal coating of Co_3O_4 nanonet. (C) Specific capacitances of carbon paper-supported Co_3O_4 nanonet and nanocube electrodes at different current densities. Reproduced with permission [97]. Copyright 2011, American Chemical Society. (D) Meyer rod coating of CNT ink on commercial Xerox paper. (E) SEM image of Xerox paper with conformal CNT coating. Reproduced with permission [98]. Copyright 2009, National Academy of Sciences, USA. (F) SEM image of the morphology of MnO_2 nanoflower deposited on CNT-paper. Inset displays the flexibility of the MnO_2-CNT-paper composite electrode. Reproduced with permission [99]. Copyright 2010, ELSEVIER.

To further increase the specific surface area for loading functional materials, Fisher *et al.* developed a carbon nanofoam hierarchical structure based on carbon paper, and hybrid EC electrode material prepared by loading MnO_2 onto the carbon nanofoam substrate was also been investigated [100]. The carbon nanofoam was fabricated by pyrolysis of carbon paper-supported resorcinol-formaldehyde nanofoam at 1,000 ^oC under inert gas. MnO_2 was subsequently loaded through a self-limiting electroless deposition method and controlled permanganate self-decomposition under a neutral pH condition. The resulting MnO_2-carbon nanofoam hybrid material maintained a highly porous structure with pore sizes mostly in the range of 10-60 nm. When tested in an aqueous 1 M Na_2SO_4 electrolyte at a scan rate of 2 mV s^{-1}, the MnO_2-carbon nanofoam revealed a specific capacitance of 110 F g^{-1} and an areal capacitance of 1.5 F cm^{-2}. These

values were further pushed to 150 F g^{-1} and 7.5 F cm^{-2} by optimizing the pore sizes and increasing the sample thickness [101].

4.2 Conventional Paper Substrate

Paper has been applied to record information for thousands of years in the human history. As a cheap and recyclable material, various papers are widely used in our daily life for wiping, packaging, and decorating. In addition, applications of paper have been expanded to flexible electronic devices, such as photodiodes, transistors, circuits, and displays [102-105]. Recently, several studies demonstrate that paper also can be an excellent support for loading active materials to fabricate high performance ECs [98, 99, 106].

One example is the CNT-paper composite reported by Hu *et al*. Single-walled carbon nanotubes (SWCNTs) were first dispersed in an aqueous solution assisted by surfactants, forming the CNT ink. Subsequently, CNT ink was applied onto a piece of commercial Xerox paper by a simple and scalable Meyer rod coating method (Figure 12D) [98]. Figure 12E shows an SEM image of Xerox paper with conformal CNT coating. With the CNT coating, the paper became highly conductive with a sheet resistance around 10 Ω/sq. The CNT coating was conformal and very stable. No CNTs fell off when the CNT-paper was flushed with water or in a Scotch tape test. The conformal coating and strong binding between CNTs and paper are attributed to large capillary effect, maximized contact area, and strong Van der Waals force. This CNT-paper composite was directly applied as both active electrodes and current collectors in ECs, in which a piece of plain paper functioned as a separator. With a CNT loading of 72 μg cm^{-2}, a high specific capacitance of 200 F g^{-1} (based on CNT mass only) was achieved in a sulfuric acid electrolyte. The highest

specific power and energy reported in the paper were 200 kW kg^{-1} and 47 W h kg^{-1}, respectively, when the EC operated at 3 V in an organic electrolyte. These all-paper ECs exhibited excellent cycling performance with only 3% (in sulfuric acid electrolyte) and 0.6% (in organic electrolyte) capacitance losses after 40,000 cycles. An even simpler EC design was realized by coating CNTs on both side of a single piece of paper [107]. PVDF pretreatment was applied on paper to block the micron-sized pores to avoid short circuiting due to CNT penetration. However, the PVDF coating may also block electrolyte to the CNT surface, resulting in a lower specific capacitance (33 F g^{-1}). Besides Meyer rod coating, Hu *et al*. also investigated an even more scalable coating method, ink-jet printing, to prepare the CNT-paper composite [107].

Kang *et al.* synthesized a similar CNT-paper composite by coating CNTs onto paper through a straightforward drop-casting method [99]. Subsequently, they deposited MnO_2 onto the CNT-paper electrochemically by running cyclic voltammetries (CVs) in an aqueous solution containing 0.1 M Na_2SO_4 and 0.1 M $Mn(CH_3COO)_2$. As shown in Figure 12F, MnO_2 was deposited on the CNT-paper surface, forming a flower-like nanostructure. The whole CNT-paper was still flexible after MnO_2 decoration (Figure 12F, inset). Loading of MnO_2 was controlled by the number of the CV cycles. Tested at a current density of ~1 A g^{-1} in a 0.1 M Na_2SO_4 aqueous electrolyte, an MnO_2-CNT-paper based EC with an MnO_2 loading of 0.38 mg cm^{-2} revealed a specific capacitance of ~540 F g^{-1}, normalized to the total mass of CNTs and MnO_2, or ~710 F g^{-1}, when considering the mass of MnO_2 only. At a current density of 5 A g^{-1}, the specific power and specific energy reported were 1,500 W kg^{-1} and 20.5 W h kg^{-1}, respectively. Higher specific

power (1,900 W kg^{-1}) was achieved at higher current density (12 A g^{-1}), while higher specific energy (43.3 W h kg^{-1}) was obtained at lower current density (1 A g^{-1}).

Zheng *et al.* reported ECs based on graphene-paper composite material, prepared by directly drawing multilayer graphenes onto commercial Xerox paper or self-made paper using graphite rods or pencils [106]. Tested in a sulfuric acid electrolyte, the specific capacitances achieved were 12 F g^{-1} for the Xerox paper and 23 F g^{-1} for the self-made paper. The relatively good electrochemical performance of the self-made paper was attributed to the more uniform surface texture and the resulting smaller and thinner graphitic flakes. The graphene-paper based EC retained ~90% capacity after 15,000 cycles, showing the desirable cycling performance.

4.3 Textile Substrate

Textile, or cloth, is a highly flexible and porous material produced from natural or synthetic fibers by pressing, weaving, knitting, or felting. Applications of textile include clothing, furnishing, cleaning, and wrapping. Depends on different fabrication processes, textile exhibits various mechanical properties. Besides flexible and lightweight, textile can also be stretchable, making it a promising substrate for wearable energy devices. Additionally, compared to paper, textile is more like a 3D structure with open pore structures. Therefore, textile can enable a 3D coating throughout the entire textile network, on both outer and inner fibers, resulting in a much higher areal mass loading of active materials, and consequently higher areal power and energy density.

With the same CNT ink applied to CNT-paper, Hu *et al.* fabricated a CNT-textile composite by a simple dipping-and-drying method: a piece of textile was dipped into

CNT ink, taken out and dried (Figure 13A) [108]. This dipping-and-drying process was repeated to increase the CNT loading to improve the conductivity of the CNT-textile composite. CNT coating conformally follow the original morphology of the textile fibers (Figure 13B). With a ~200-nm-thick CNT coating, the textile fiber (~20 μm in diameter) achieved a conductance of 50 S cm^{-1}, considering the volume of both the textile fiber core and the CNT coating shell [109]. The sheet resistance of the CNT-textile could be less than 1 Ω/sq after nitric acid treatment. In an organic electrolyte with 1 M $LiPF_6$, ECs based on the CNT-textile with a CNT loading of 0.24 mg cm^{-2} were tested by galvanostatic cycling with current densities varying from 20 μA cm^{-2} to 20 mA cm^{-2}. The specific capacitance achieved were 140 F g^{-1} and 80 F g^{-1}, respectively. Compared to a flat CNT-polyethylene terephthalate (PET) composite with the same CNT loading, the CNT-textile revealed 2-3 times higher specific capacitance. Higher CNT mass loading up to 8 mg cm^{-2} was investigated, resulting in an elevated areal capacitance of 0.48 F cm^{-2}. Because of the lightweight of textile (~12 mg cm^{-2}) and avoiding metal current collector, the total mass of a CNT-textile-based EC was only 48 mg cm^{-2}, in which the active material, CNTs, accounts for more than 30%. Calculated based on the total mass, the CNT-textile-based ECs achieved outstanding specific power (10 kW kg^{-1}) and specific energy (20 W h kg^{-1}), compared to commercial ECs. In terms of the long term cycling performance, the specific capacitance of a CNT-textile-based EC maintained within 2% variation during 130,000 cycles. Another study tested the performance of the CNT-textile-based ECs in an aqueous electrolyte with 2 M Li_2SO_4, revealing a high specific capacitance of ~70-80 F g^{-1} and good cycling stability up to 35,000 cycles [110].

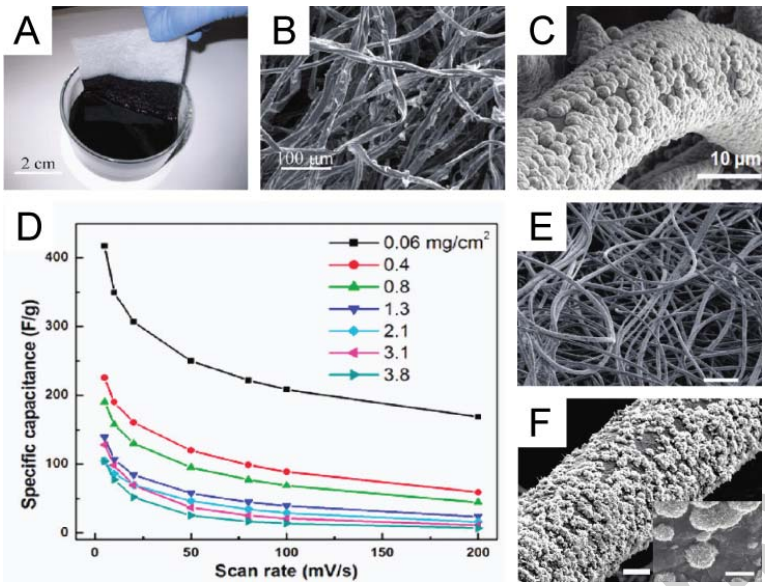

Figure 13 Textile-based ECs. (A) Dipping a piece of textiles into an aqueous CNT ink. (B) SEM image of CNT-coated textile reveals the macroporous structure. Reproduced with permission [104]. Copyright 2010, American Chemical Society. (C) SEM of MnO_2-CNT-textile. (D) Specific capacitances at different scan rates for MnO_2-CNT-textile samples with different areal mass loading of MnO_2. Reproduced with permission [111]. Copyright 2011, American Chemical Society. (E) SEM image of a sheet of graphene-coated textile with MnO_2 modification showing large-scale, uniform deposition of MnO_2 nanomaterials achieved on almost entire fabric fiber surfaces. Scale bar: 200 μm. (F) SEM image of a typical microfiber with conformal coating of MnO_2 nanostructures. Inset shows a SEM image of the nanoflower structure of electrodeposited MnO_2 particles. Scale bars are 5 and 1 μm for main figure and inset. Reproduced with permission[112]. Copyright 2011, American Chemical Society.

The highly conductive and open porous CNT-textile provides an effective 3D support for deposition of other active functional materials, such as catalyst [1113], battery electrode materials [114], and pseudocapacitor materials [111]. Hu *et al.* electrochemically deposited MnO_2 onto CNT-textile by applying a negative current of 500 μA cm^{-2} in an aqueous electrolyte containing 100 mM Na_2SO_4 and 10 mM $MnSO_4$ for 5-600 minutes, corresponded to MnO_2 loadings of 0.06-8.3 mg cm^{-2} [111]. As shown in Figure 13C, nanoflower-like MnO_2 particles were deposited onto the CNT-coated textile fibers uniformly. Even with a high MnO_2 loading of 8.3 mg cm^{-2}, the composite still maintained a porous structure. Performance of the ECs prepared with this MnO_2-

CNT-textile composite was evaluated in an aqueous Na_2SO_4 (0.5 M) electrolyte. Specific capacitance at different scan rates for MnO_2-CNT-textile samples with different areal mass loading of MnO_2 was shown in Figure 13D. The highest specific capacitance achieved was 410 F g^{-1}, with a MnO_2 loading of 0.06 mg cm^{-2} at a scan rate of 5 mV s^{-1}; while the highest areal capacitance obtained was 2.8 F cm^{-2}, when the mass loading was 8.3 mg cm^{-2} and the scan rate was low at 0.05 mV s^{-1}. To demonstrated the advantages of the CNT-textile as a 3D support, 0.8 mg cm^{-2} MnO_2 was deposited on both a piece of CNT-textile and a flat Pt foil. At a scan rate of 5 mV s^{-1}, the specific capacitance of MnO_2 on the CNT-textile support was 10 times more than that on the Pt support (185 F g^{-1} vs. 18 F g^{-1}). Additionally, the conformal MnO_2 coating on CNT-textile fibers was fairly stable, while the MnO_2 film on Pt was fragile and easily cracked into pieces. The authors assembled a pouch cell with MnO_2-CNT-textile as the positive electrode and reduced MnO_2-CNT-textile as the negative electrode, achieving a specific power ~13 kW kg^{-1} and s specific energy ~5-20 W h kg^{-1}. However, this EC exhibited a poor cycling performance: 20% capacitance lost after 200 cycles and 40% lost after 10,000 cycles. The failure was possibly due to the loss of active materials and the mismatched capacity between the two electrodes. Another hybrid textile-based EC was prepared by ink-jet printing CNTs on cloth fabrics and drop casting RuO_2 nanowires subsequently [115]. The achieved specific capacitance, specific power and specific energy were 138 F g^{-1}, 96 kW kg^{-1}, and 18.8 W h kg^{-1}, respectively.

To reduce the cost of textile-based ECs for potentially large-scale energy storage systems, graphene materials have been explored to replace CNTs. Graphene nanosheets were loaded on the textile, forming conductive graphene/textile composite [112].

Graphene ink was prepared through a low-cost and high-throughput solution-based exfoliation technique. Graphene-textile and MnO_2-graphene-textile were fabricated subsequently by dip coating and electrodeposition, respectively, similar to the procedures applied to synthesize CNT-textile and MnO_2-CNT-textile described above. Large-scale, uniform deposition of MnO_2 nanomaterials achieved on almost entire textile fiber surfaces (Figure 13E and 13F). Tested in an aqueous electrolyte (0.5 M Na_2SO_4) at a scan rate of 2 mV s^{-1}, the MnO_2-graphene-textile with a MnO_2 loading of ~0.3 mg cm^{-2} achieved a specific capacitance of ~315 F g^{-1}, which is ~5 times higher than that of the plain graphene-textile. An asymmetric EC was assembled with MnO_2-graphene-textile as the positive electrode and CNT-textile as the negative electrode. When operated at 1.5 V, the asymmetric ECs achieved a specific power of 110 kW kg^{-1}, a specific energy of 12.5 W h kg^{-1}, and good cycling performance of ~95% capacitance retention over 5,000 cycles.

4.4 Sponge Substrate

Synthetic sponge, fabricated from various polymers, is also a low-cost abundant daily life material commonly used for household cleaning, packaging, furniture padding, etc. Similar to textile, sponge also shows an open macroporous structure readily for 3D coating of active materials. In addition, sponge possesses the following advantages: (1) 3D interconnected frame work enables continuous coating without any interruption; (2) uniform and tunable pore size can be well controlled by the manufacture process; and (3) isotropic mechanical property overcomes the limit in thickness for other layered structures, like textile [116]. These unique properties of sponge suggest it an excellent supporting substrate for loading active materials.

CNT-sponge composite was prepared by the same "dipping-and-drying" method. The conformal CNT coating layer was continuous in all three dimensions (**Figure 14A**). With a 200-nm-thick CNT coating, the conductance of CNT-sponge reached ~1 S cm^{-1}, treated as a solid conductor. With the pore size in a range of 300-500 μm, the porosity and specific surface area of CNT-sponge were ~98% and 10^4 m^2 m^{-3}, respectively. The CNT-sponge inherited excellent physical and mechanical properties from original sponge, including lightweight, flexible, stretchable, and compressible [116]. ECs built with two pieces of symmetrical CNT-sponge (1 cm × 1 cm × 0.1 cm) were investigated in an aqueous 1 M Na_2SO_4 electrolyte [117]. A wide range scan rate of 0.001-200 V s^{-1} was conducted in the CV test and the resulting curves retain a rectangular shape at a scan rate up to 20 V s^{-1}. The results also revealed a linear dependence of discharge current on the scan rate up to 8 V s^{-1}. Operated at a scan rate of 10 V s^{-1}, only 2% degradation of specific capacitance was observed after 100,000 cycles (Figure 14D). MnO_2 was further loaded on CNT-sponge by electrochemical deposition to improve the energy density of the whole device. Figure 14B shows a picture of a MnO_2-CNT-sponge composite electrode, suggesting its flexible feature. When a MnO_2-CNT-sponge sample with ~0.03 mg cm^{-2} MnO_2 was tested at a scan rate of 1 mV s^{-1}, the specific capacitance of MnO_2 reached ~1,230 F g^{-1}, which was very close to the theoretical limit (Figure 14C). Full EC cells based on MnO_2-CNT-sponge also exhibited excellent performance: a specific power of 63 kW kg^{-1}, a specific energy of 31 W h kg^{-1}, and only 4% capacitance loss after 10,000 cycles (Figure 14D).

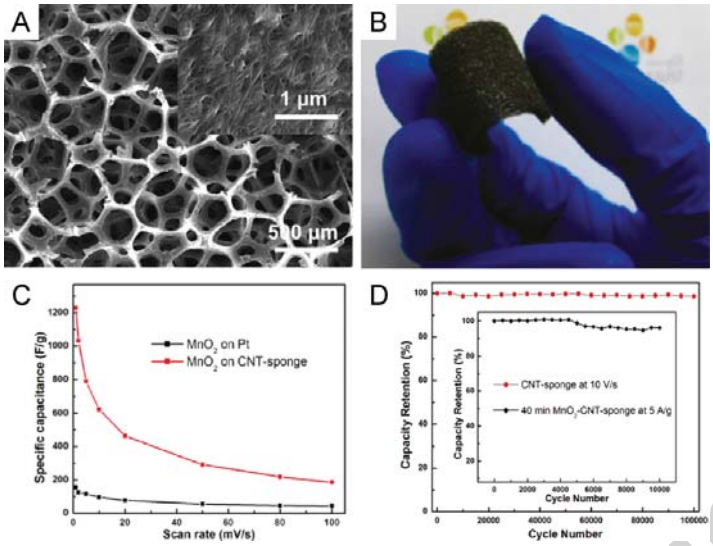

Figure 14 Sponge-based ECs. (A) SEM image of the CNT coated sponge showing macroscale porous structure. Reproduced with permission [112]. Copyright 2011, The Royal Society of Chemistry. (B) Photograph of a MnO_2-CNT-sponge electrode. (C) Specific capacitance of MnO_2-CNT-sponge and MnO_2-Pt (all based on the mass of MnO_2). (D) Capacity retention vs. cycle number for CNT-sponge and MnO2-CNT-sponge supercapacitors. Reproduced with permission [117]. Copyright 2011, American Chemical Society.

Conclusion and Perspective

Today ECs have emerged as a promising energy storage technology. Great advancements have been made recently in developing new electrode materials including nanoporous carbons with proper pore size control down to angstrom accuracy, new categories of carbon materials with much higher surface areas such as CNTs and graphene, and pseudocapacitive metal oxide nanomaterials and conducting polymers that can offer high energy density. Most recently, exciting progress has also been made in exploring hybrid nanostructured materials that combine both advantages of EDLCs and pseudocapacitors for further improved energy density while maintaining high power capability. To ultimately realize both high power and high energy density, novel support structures have been developed for high mass loading of active materials and effective utilization of their

electrochemical properties, including synthetically engineered carbon nano-networks, and low-cost porous paper, textile, and sponge substrates that offer great promise for developing large-scale energy storage systems.

Currently the primary challenges for EC technology are the limited energy density and the relatively high cost of ECs, hindering them being the energy storage technology of choice for many applications.[9] Despite their high level of power performance, ECs are still simply too expensive to compete against the other available EES systems such as batteries. It should be also noted that lowering the cost must be done without sacrificing the long cycle life and exceptional high rate performance that distinguishes ECs from batteries.

Improving the energy density of ECs can be achieved by designing new hybrid electrode materials to combine EDL capacitance together with fast and highly reversible pseudocapacitance, by using ionic liquid electrolytes with a stable electrochemical voltage window >4 V, and by developing hybrid EC systems to optimize the potential range for each electrode so as to widen the overall cell voltage. Increasing the voltage at which the EC can operate reliably is one of the most effective ways to enhance both energy density and power density given the relation of the V^2 term to both E (energy) and P (power). Herein further development of relatively low-cost electrolytes that can offer both large EC operational voltage window and good ionic conductivity is still needed.

As for developing hybrid material system for EC electrodes, more research efforts should be placed on understanding two levels of interface, namely the interface between electrolyte and pseudocapacitor materials and the interface within the hybrid between carbon material and the pseudocapacitive material. The key challenge remains to

enhancing the interactions between carbon and the pseudocapacitive material to improve the Faradic processes across the interface so as to achieve efficient pseudocapacitance in addition to the EDL capacitance, as well as to sustain the strain caused by phase/volume change for long cycle life.

The greatest challenge for popularizing EC technology, especially for large-scale energy storage applications, is the high cost of EC devices. There are two key aspects when designing electrode materials and structures to meet these requirements of future generation ECs: inexpensive yet high-performance materials with rationally designed architectures and scalable processing for low-cost fabrication. From the point of view of materials, a promising strategy would be incorporating earth-abundant capacitive carbon materials with low-cost pseudocapacitive metal oxides such as MnO_2. In addition, from the perspective of the fabrication process, highly scalable approaches to make functional electrodes and construct ECs, such as facile solution-based process and printing technique, will be of great importance to provide a long-term solution for making large-scale and low-cost devices. For example, aqueous asymmetric ECs are a promising system for the next-generation EC technology due to their potential for enhanced specific energy, reduced costs, and safer cell chemistries compared to present EDLCs. Such EC system can further bridge the energy/power performance gap between conventional batteries and EDLCs in a form that offers significant advantages in terms of cost and safety.[24]

Looking forward, EC technology will play a bigger role in energy storage and harvesting, helping decrease the total energy consumption and minimize the use of hydrocarbon fuels. Moreover, flexible, printable and wearable ECs are likely to be

integrated into smart clothing, sensors, and other wearable electronics. In some instances they will replace batteries, but in many cases they will either complement batteries, increasing their efficiency and lifetime, or serve as energy solutions where an extremely large number of cycles, long lifetime and fast power delivery are required.

Acknowledgement

Y. Cui and Z. Bao acknowledge the financial support from the Precourt Institute for Energy at Stanford University. Y. Cui also acknowledges the funding support from the King Abdullah University of Science and Technology (KAUST) Investigator Award (No. KUS-l1-001-12), and from the Department of Energy, Office of Basic Energy Sciences, Division of Materials Sciences and Engineering under contract DE-AC02-76SF00515 through the SLAC National Accelerator Laboratory LDRD project. L. Pan acknowledges the financial support from National Science foundation of China (No. 61076017).

References

[1] D. Ginley, M.A. Green, R. Collins, MRS Bulletin 33 (2008) 355.
[2] V.S. Arunachalam, E.L. Fleischer, MRS Bulletin 33 (2008) 264.
[3] J.P. Holdren, Science 315 (2007) 737.
[4] M. Winter, R.J. Brodd, Chemical Reviews 104 (2004) 4245.
[5] Z. Yang, J. Zhang, M.C.W. Kintner-Meyer, X. Lu, D. Choi, J.P. Lemmon, J. Liu, Chemical Reviews 111 (2011) 3577.
[6] B.E. Conway, *Electrochemical Supercapacitors: Scientific Fundamentals and Technological Applications*. Kluwer Academic/Plenum: New York, 1999
[7] A. Burke, Journal of Power Sources 91 (2000) 37.
[8] D.R. Rolison, L.F. Nazar, MRS Bulletin 36 (2011) 486.
[9] J.R. Miller, A.F. Burke, Electrochem. Soc. Interf. 17 (2008) 53.
[10] P. Simon, Y. Gogotsi, Nature Materials 7 (2008) 845.
[11] J.R. Miller, P. Simon, Science 321 (2008) 651.
[12] P.J. Hall, M. Mirzaeian, S.I. Fletcher, F.B. Sillars, A.J.R. Rennie, G.O. Shitta-Bey, G. Wilson, A. Cruden, R. Carter, Energy & Environmental Science 3 (2010) 1238.
[13] A. Burke, International Journal of Energy Research 34 (2010) 133.
[14] L.F. Nazar, G. Goward, F. Leroux, M. Duncan, H. Huang, T. Kerr, J. Gaubicher, Int. J. Inorg. Mater. 3 (2001) 191.
[15] M. Hirscher, Materials Science and Engineering B 108 (2004) 1.
[16] A.S. Arico, P. Bruce, B. Scrosati, J.-M. Tarascon, W. van Schalkwijk, Nature Materials 4 (2005) 366.
[17] M.D. Stoller, R.S. Ruoff, Energy & Environmental Science 3 (2010) 1294.
[18] Y. Gogotsi, P. Simon, Science 334 (2011) 917.
[19] C. Liu, Z. Yu, D. Neff, A. Zhamu, B.Z. Jang, Nano Letters 10 (2010) 4863.
[20] J. Huang, B.G. Sumpter, V. Meunier, Angew. Chem., Int. Ed. 47 (2008) 520.
[21] T. Cottineau, M. Toupin, T. Delahaye, T. Brousse, D. Bélanger, Applied Physics A 82 (2006) 599.
[22] D. Bélanger, T. Brousse, J.W. Long, Electrochem. Soc. Interfaces 17 (2008) 49.
[23] K. Naoi, M. Morita, Electrochem. Soc. Interfaces 17 (2008) 44.
[24] J.W. Long, D. Belanger, T. Brousse, W. Sugimoto, M.B. Sassin, O. Crosnier, MRS Bulletin 36 (2011) 513.
[25] J. Biener, M. Stadermann, M. Suss, M.A. Worsley, M.M. Biener, K.A. Rose, T.F. Baumann, Energy & Environmental Science 4 (2011) 656.
[26] M. Kaempgen, C.K. Chan, J. Ma, Y. Cui, G. Gruner, Nano Letters 9 (2009) 1872.
[27] A. Izadi-Najafabadi, S. Yasuda, K. Kobashi, T. Yamada, D.N. Futaba, H. Hatori, M. Yumura, S. Iijima, K. Hata, Advanced Materials 22 (2010) E235.
[28] J. Chmiola, C. Largeot, P.-L. Taberna, P. Simon, Y. Gogotsi, Science 328 (2010) 480.
[29] D. Pech, M. Brunet, H. Durou, P.H. Huang, V. Mochalin, Y. Gogotsi, P.L. Taberna, P. Simon, Nature Nanotechnology 5 (2010) 651.
[30] M.D. Stoller, S. Park, Y. Zhu, J. An, R.S. Ruoff, Nano Letters 8 (2008) 3498.
[31] A.G. Pandolfo, A.F. Hollenkamp, Journal of Power Sources 157 (2006) 11.

[32] L.L. Zhang, X.S. Zhao, Chemical Society Reviews 38 (2009) 2520.
[33] E. Frackowiak, Phys. Chem. Chem. Phys. 9 (2007) 1774.
[34] S.W. Lee, B.M. Gallant, H.R. Byon, P.T. Hammond, Y. Shao-Horn, Energy & Environmental Science 4 (2011) 1972.
[35] Y.W. Zhu, S. Murali, M.D. Stoller, K.J. Ganesh, W.W. Cai, P.J. Ferreira, A. Pirkle, R.M. Wallace, K.A. Cychosz, M. Thommes, D. Su, E.A. Stach, R.S. Ruoff, Science 332 (2011) 1537.
[36] C.-C. Hu, K.-H. Chang, M.-C. Lin, Y.-T. Wu, Nano Letters 6 (2006) 2690.
[37] V. Subramanian, S.C. Hall, P.H. Smith, B. Rambabu, Solid State Ionics 175 (2004) 511.
[38] D.-W. Wang, F. Li, H.-M. Cheng, Journal of Power Sources 185 (2008) 1563.
[39] K. Naoi, P. Simon, Electrochem. Soc. Interf. 17 (2008) 34.
[40] J.P. Zheng, P.J. Cygan, T.R. Jow, Journal of the Electrochemical Society 142 (1995) 2699.
[41] H.Y. Lee, J.B. Goodenough, Journal of Solid State Chemistry 144 (1999) 220.
[42] A. Rudge, J. Davey, I. Raistrick, S. Gottesfeld, J. Ferraris, Journal of Power Sources 47 (1994) 89.
[43] S.R. Sivakkumar, W.J. Kim, J.-A. Choi, D.R. MacFarlane, M. Forsyth, D.-W. Kim, Journal of Power Sources 171 (2007) 1062.
[44] Z.S. Wu, W. Ren, D.W. Wang, F. Li, B. Liu, H.M. Cheng, ACS Nano 4 (2010) 5835.
[45] P.-C. Chen, G. Shen, Y. Shi, H. Chen, C. Zhou, ACS Nano 4 (2010) 4403.
[46] B.E. Conway, V. Birss, J. Wojtowicz, Journal of Power Sources 66 (1997) 1.
[47] Z. Wu, G. Zhou, L. Yin, W. Ren, F. Li, H. Cheng, Nano Energy 1 (2012) 107.
[48] X. Li, B. Wei, Nano Energy 1 (2012) 479.
[49] J. Liu, J. Essner, J. Li, Chemistry of Materials 22 (2010) 5022.
[50] M.S. Wu, Z.S. Guo, J.J. Jow, Journal of Physical Chemistry C 114 (2010) 21861.
[51] G.R. Li, Z.P. Feng, Y.N. Ou, D.C. Wu, R.W. Fu, Y.X. Tong, Langmuir 26 (2010) 2209.
[52] Y.H. Lin, T.Y. Wei, H.C. Chien, S.Y. Lu, Advanced Energy Materials 1 (2011) 901.
[53] Y.T. Peng, Z. Chen, J. Wen, Q.F. Xiao, D. Weng, S.Y. He, H.B. Geng, Y.F. Lu, Nano Research 4 (2011) 216.
[54] S. Chen, J. Zhu, X. Wu, Q. Han, X. Wang, ACS Nano 4 (2010) 2822.
[55] H. Zhang, G.P. Cao, Z.Y. Wang, Y.S. Yang, Z.J. Shi, Z.N. Gu, Nano Letters 8 (2008) 2664.
[56] S.W. Lee, J. Kim, S. Chen, P.T. Hammond, Y. Shao-Horn, ACS Nano 4 (2010) 3889.
[57] J.H. Kim, K.H. Lee, L.J. Overzet, G.S. Lee, Nano Letters 11 (2011) 2611.
[58] J.T. Zhang, J.W. Jiang, X.S. Zhao, Journal of Physical Chemistry C 115 (2011) 6448.
[59] J.S. Ye, H.F. Cui, X. Liu, T.M. Lim, W.D. Zhang, F.S. Sheu, Small 1 (2005) 560.
[60] A.L.M. Reddy, S. Ramaprabhu, Journal of Physical Chemistry C 111 (2007) 7727.
[61] A. Ghosh, E.J. Ra, M. Jin, H.-K. Jeong, T.H. Kim, C. Biswas, Y.H. Lee, Advanced Functional Materials 21 (2011) 2541.
[62] W.-C. Fang, Journal of Physical Chemistry C 112 (2008) 11552.

[63] H. Wang, H.S. Casalongue, Y. Liang, H. Dai, Journal of the American Chemical Society 132 (2010) 7472.
[64] Y.Y. Liang, M.G. Schwab, L.J. Zhi, E. Mugnaioli, U. Kolb, X.L. Feng, K. Mullen, Journal of the American Chemical Society 132 (2010) 15030.
[65] L. Pan, H. Qiu, C. Dou, Y. Li, L. Pu, J. Xu, Y. Shi, Inter. J. Mol. Sci. 11 (2010) 2636.
[66] M.J. Bleda-Martinez, C. Peng, S. Zhang, G.Z. Chen, E. Morallon, D. Cazorla-Amoros, Journal of the Electrochemical Society 155 (2008) A672.
[67] J. Jang, J. Bae, M. Choi, S.H. Yoon, Carbon 43 (2005) 2730.
[68] X. Yan, Z. Tai, J. Chen, Q. Xue, Nanoscale 3 (2011) 212.
[69] Z. Lei, Z. Chen, X.S. Zhao, J. Phys. Chem. C 114 (2010) 19867.
[70] L.L. Zhang, S. Li, J. Zhang, P. Guo, J. Zheng, X.S. Zhao, Chemistry of Materials 22 (2010) 1195.
[71] I. Kovalenko, D.G. Bucknall, G. Yushin, Advanced Functional Materials 20 (2010) 3979.
[72] Y.G. Wang, H.Q. Li, Y.Y. Xia, Advanced Materials 18 (2006) 2619.
[73] L. Fan, Y. Hu, J. Maier, P. Adelhelm, B. Smarsly, M. Antonietti, Advanced Functional Materials 17 (2007) 3083.
[74] Y.-Y. Horng, Y.-C. Lu, Y.-K. Hsu, C.-C. Chen, L.-C. Chen, K.-H. Chen, Journal of Power Sources 195 (2010) 4418.
[75] L. Li, H. Song, Q. Zhang, J. Yao, X. Chen, Journal of Power Sources 187 (2009) 268.
[76] M.N. Hyder, S.W. Lee, F.C. Cebeci, D.J. Schmidt, Y. Shao-Horn, P.T. Hammond, ACS Nano 5 (2011) 8552.
[77] J. Liu, J. Sun, L. Gao, J. Phys. Chem. C 114 (2010) 19614.
[78] J. Ge, G. Cheng, L. Chen, Nanoscale 3 (2011) 3084.
[79] Y. Zhao, H. Bai, Y. Hu, Y. Li, L. Qu, S. Zhang, G. Shi, Journal of Materials Chemistry 21 (2011) 13978.
[80] L. Lai, L. Wang, H. Yang, N. G. Sahoo, Q. X. Tam, J. Liu, C. K. Poh, S. H. Lim, Z. Shen, Ji. Lin, Nano Energy 1 (2012) 723.
[81] G. Zhou, D. Wang, F. Li, L. Zhang, Z. Weng, H. Cheng, New Carbon Materials 26 (2011) 180.
[82] X.M. Feng, R.M. Li, Y.W. Ma, R.F. Chen, N.E. Shi, Q.L. Fan, W. Huang, Advanced Functional Materials 21 (2011) 2989.
[83] A. Davies, P. Audette, B. Farrow, F. Hassan, Z. Chen, J.-Y. Choi, A. Yu, Journal of Physical Chemistry C 115 (2011) 17612.
[84] J. An, J. Liu, Y. Ma, R. Li, M. Li, M. Yu, S. Li, European Physical Journal-Applied Physics 58 (2012) 30403.
[85] Y. Hou, Y. Cheng, T. Hobson, J. Liu, Nano Letters 10 (2010) 2727.
[86] G. Yu, L. Hu, N. Liu, H. Wang, M. Vosgueritchian, Y. Yang, Y. Cui, Z. Bao, Nano Letters 11 (2011) 4438.
[87] V. Augustyn, B. Dunn, Comptes Rendus Chimie 13 (2010) 130.
[88] K. Brezesinski, J. Wang, J. Haetge, C. Reitz, S.O. Steinmueller, S.H. Tolbert, B.M. Smarsly, B. Dunn, T. Brezesinski, Journal of the American Chemical Society 132 (2010) 6982.

[89] T. Brezesinski, J. Wang, J. Polleux, B. Dunn, S.H. Tolbert, Journal of the American Chemical Society 131 (2009) 1802.
[90] J. Wang, J. Polleux, J. Lim, B. Dunn, Journal of Physical Chemistry C 111 (2007) 14925.
[91] X. Lang, A. Hirata, T. Fujita, M. Chen, Nature Nanotechnology 6 (2011) 232.
[92] X.P. Dong, W.H. Shen, J.L. Gu, L.M. Xiong, Y.F. Zhu, Z. Li, J.L. Shi, Journal of Physical Chemistry B 110 (2006) 6015.
[93] H. Li, R. Wang, R. Cao, Microporous and Mesoporous Materials 111 (2008) 32.
[94] J. Chen, J.Z. Wang, A.I. Minett, Y. Liu, C. Lynam, H. Liu, G.G. Wallace, Energy & Environmental Science 2 (2009) 393.
[95] S. Park, B.N. Popov, Fuel 90 (2011) 436.
[96] E.J. Ra, E. Raymundo-Pinero, Y.H. Lee, F. Beguin, Carbon 47 (2009) 2984.
[97] L. Yang, S. Cheng, Y. Ding, X. Zhu, Z.L. Wang, M. Liu, Nano Letters 12 (2012) 321.
[98] L. Hu, J.W. Choi, Y. Yang, S. Jeong, F. La Mantia, L.-F. Cui, Y. Cui, Proc. Natl. Acad. Sci. U.S.A. 106 (2009) 21490.
[99] Y.J. Kang, B. Kim, H. Chung, W. Kim, Synthetic Metals 160 (2010)
[100] A.E. Fischer, K.A. Pettigrew, D.R. Rolison, R.M. Stroud, J.W. Long, Nano Letters 7 (2007) 281.
[101] J.C. Lytle, J.M. Wallace, M.B. Sassin, A.J. Barrow, J.W. Long, J.L. Dysart, C.H. Renninger, M.P. Saunders, N.L. Brandell, D.R. Rolison, Energy & Environmental Science 4 (2011) 1913.
[102] P. Andersson, D. Nilsson, P.O. Svensson, M.X. Chen, A. Malmstrom, T. Remonen, T. Kugler, M. Berggren, Advanced Materials 14 (2002) 1460.
[103] F. Eder, H. Klauk, M. Halik, U. Zschieschang, G. Schmid, C. Dehm, Applied Physics Letters 84 (2004) 2673.
[104] N.J. Kaihovirta, C.-J. Wikman, T. Makela, C.-E. Wilen, R. Osterbacka, Advanced Materials 21 (2009) 2520.
[105] D.-H. Kim, Y.-S. Kim, J. Wu, Z. Liu, J. Song, H.-S. Kim, Y.Y. Huang, K.-C. Hwang, J.A. Rogers, Advanced Materials 21 (2009) 3703.
[106] G. Zheng, L. Hu, H. Wu, X. Xie, Y. Cui, Energy & Environmental Science 4 (2011) 3368.
[107] L. Hu, H. Wu, Y. Cui, Applied Physics Letters 96 (2010) 183502.
[108] L. Hu, M. Pasta, F.L. Mantia, L. Cui, S. Jeong, H.D. Deshazer, J.W. Choi, S.M. Han, Y. Cui, Nano Letters 10 (2010) 708.
[109] X. Xie, L.B. Hu, M. Pasta, G.F. Wells, D.S. Kong, C.S. Criddle, Y. Cui, Nano Letters 11 (2011) 291.
[110] M. Pasta, F. La Mantia, L. Hu, H. Deshazer, Y. Cui, Nano Research 3 (2010) 452.
[111] L. Hu, W. Chen, X. Xie, N. Liu, Y. Yang, H. Wu, Y. Yao, M. Pasta, H.N. Alshareef, Y. Cui, ACS Nano 5 (2011) 8904.
[112] G. Yu, L. Hu, M. Vosgueritchian, H. Wang, X. Xie, J.R. McDonough, X. Cui, Y. Cui, Z. Bao, Nano Letters 11 (2011) 2905.
[113] X. Xie, M. Pasta, L. Hu, Y. Yang, J. McDonough, J. Cha, C.S. Criddle, Y. Cui, Energy & Environmental Science 4 (2011) 1293.
[114] L. Hu, F. La Mantia, H. Wu, X. Xie, J. McDonough, M. Pasta, Y. Cui, Advanced Energy Materials 1 (2011) 1012.

[115] P. Chen, H. Chen, J. Qiu, C. Zhou, Nano Research 3 (2010) 594.
[116] X. Xie, M. Ye, L. Hu, N. Liu, J.R. McDonough, W. Chen, H.N. Alshareef, C.S. Criddle, Y. Cui, Energy & Environmental Science 5 (2012) 5265.
[117] W. Chen, R.B. Rakhi, L. Hu, X. Xie, Y. Cui, H.N. Alshareef, Nano Letters 11 (2011) 5165.

Guihua Yu is an Assistant Professor at The University of Texas at Austin. He received his BS degree with highest honor in chemistry from University of Science and Technology of China, earned his PhD in chemistry with Professor Charles M. Lieber at Harvard University in 2009, and did his three years postdoctoral research with Professor Zhenan Bao and Professor Yi Cui at Stanford. His current research focuses on developing nanomaterials and nanostructures for energy storage and conversion devices such as supercapacitors and lithium-ion batteries, as well as novel assembly and integration of nanoelectronic devices based on carbon nanotubes and semiconductor nanowires.

Xing Xie received his B.S. (2006) and M.S. (2008) degrees from Tsinghua University, and he is now a joint graduate student in Civil & Environmental Engineering and Materials Science & Engineering at Stanford University. His current research focuses on applying nano-enhanced three-dimensional hybrid electrodes for microbial fuel cells or supercapacitors. He is a Henry Fan Fellow supported by the Stanford Interdisciplinary Graduate Fellowship.

Lijia Pan is a visiting scholar at Stanford University with Professor Zhenan Bao. He is an Associate Professor at School of Electronic Science and Engineering, Nanjing University. He received his BS degree in polymer science and engineering from South China University of Technology, obtained his PhD in polymer physics from University of Science and Technology of China in 2003, did three years postdoctoral research in physics department of Nanjing University. His research focuses on developing micro and nanostructures of conducting polymers for energy storage and sensors.

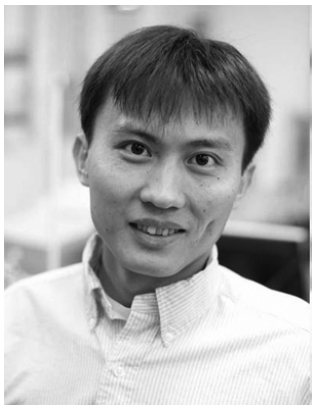

Yi Cui is an Associate Professor of Materials Science and Engineering at Stanford University. He earned his PhD degree in chemistry in 2002 from Harvard University. After postdoctoral research at the University of California, Berkeley as a Miller Fellow, Cui became an assistant professor in the Department of Materials Science and Engineering at Stanford in 2005 and was promoted to tenured associate professor in 2010. His research focuses on designing nanomaterials for energy, environmental and biological applications. Cui has received a number of awards including the Wilson Prize, the Sloan Research Fellowship, the KAUST Investigator Award, the Office of Naval Research Young Investigator Award.

Zhenan Bao is a Professor of Chemical Engineering at Stanford University. She received her PhD in Chemistry from the University of Chicago in 1995. She then joined Bell Labs and became a Distinguished Member of Technical Staff in 2001. Bao joined the faculty of Chemical Engineering in Stanford in 2004. Her research involves design and synthesis of new organic materials and processing methods for flexible and stretchable electronics. Bao is an American Chemical Society (ACS) Fellow, ACS PMSE Fellow and SPIE Fellow. She has published more than 200 scientific papers and received a number of awards, including the Arthur Cope Scholar Award and the Beilby Medal from Royal Society of Chemistry.

- We review recent progress on hybrid nanostructured electrodes for electrochemical capacitors.
- We focus on hybrid electrodes combining carbon materials with metal oxides or conducting polymers.
- We emphasize novel porous structures for high loading of electroactive nanomaterials.